Poly(*n*-butyl isocyanide): yellow-brown solid; IR (KBr) 1639 (C=N) cm⁻¹; ¹H NMR (CCl₄) δ 0.95-1.45 (br, 7 H, (CH₂)₂CH₃), 3.35 (br, 2 H, NCH₂).

Poly(3-pentyl isocyanide): pale yellow solid; IR (KBr) 1623 (C=N) cm⁻¹.

Poly(benzyl isocyanide): brown solid; IR (KBr) 1630 (C=N) cm⁻¹; ¹H NMR (CDCl₃) δ 4.0-5.0 (br, 2 H, CH₂), 6.5-7.5 (br, 5 H, ArH).

Poly(α,α-dimethylbenzyl isocyanide): pale yellow solid; IR (KBr) 1620 (C=N) cm⁻¹; ¹H NMR (CDCl₃) δ 2.60 (br, 6 H, CH₃), 6.3 (br, 5 H, ArH).

Poly(phenyl isocyanide): yellow solid; IR (KBr) 1643 (C=N) cm⁻¹; ¹H NMR (CCl₄) δ 6.35 (br, ArH).

Poly(4-methoxyphenyl isocyanide): yellow solid; IR (KBr) 1630 (C=N) cm⁻¹; ¹H NMR (CCl₄) δ 3.25-3.70 (br, 3 H, CH), 6.30 (br, 4 H, ArH).

Poly(4-methoxy-2-methylphenyl isocyanide): yellow solid; IR (KBr) 1630 (C=N) cm⁻¹; ¹H NMR (CDCl₃) δ 0-2.0 (br, 3 H, CH₃), 2.5-4.0 (br, 3 H, OCH₃), 5.0-7.0 (br, 3 H, ArH).

Poly(2,6-difluorophenyl isocyanide): yellow solid; IR (KBr) 1650 (C=N) cm⁻¹.

Poly(2,6-dichlorophenyl isocyanide): yellow solid; IR (KBr) 1630 (C=N) cm⁻¹.

Poly(2-*tert*-butylphenyl isocyanide): yellow solid; IR (KBr) 1618 (C=N) cm⁻¹.

Poly(2-biphenyl isocyanide): yellow solid; IR (KBr) 1615 (C=N) cm⁻¹; ¹H NMR (CDCl₃) δ ≈ 7 (br, ArH).

Poly[4-(dimethylamino)phenyl isocyanide]: yellow-brown solid; IR (KBr) 1605 (C=N) cm⁻¹.

Polymerization in the Presence of Chiral Additives Other Than Chiral Amines. In a typical procedure, 4-methoxyphenyl isocyanide (220 mg, 1.65 mmol), anhydrous NiCl₂ (1.2 mg, 9.2 × 10⁻³ mmol), and (*S,S*)-chiraphos [2*S*,3*S*-(-)-bis(diphenylphosphino)butane; 44.4 mg, 0.10 mmol] were stirred in CHCl₃ (2 mL) for 12 h at ambient temperature. The mixture was concentrated, and added to excess methanol. The precipitate was isolated by filtration, washed with methanol, and dried under vacuum at 50 °C; yield 138.2 mg (63%) of poly(4-methoxyphenyl isocyanide). The polymer showed no optical rotation and had physical properties as described above.

Similar experiments were carried out under various conditions using 1-borneol, cinchonine, (*R,R*)-DIOP, neomenthyldiphenylphosphine, and (2*S*,2′*S*)-2-(hydroxymethyl)-1-[(methylpyrrolidin-2-yl)methyl]-pyrrolidine as additives. Polymer yields amounted to 60-70%. None of the polymers showed optical rotation.

Registry No. **1e**, 608-31-1; **1f**, 585-32-0; **1g**, 24544-04-5; **1h**, 6310-21-0; **11**, 102-50-1; **1o**, 14227-17-9; **2a**, 871-71-6; **2b**, 59734-20-2; **2c**, 2425-74-3; **2d**, 23602-10-0; **2e**, 10113-35-6; **2f**, 42044-69-9; **2g**, 84250-69-1; **2h**, 99858-67-0; **2i**, 6343-54-0; **2l**, 7402-54-2; **2m**, 18606-63-8; **2n**, 5346-21-4; **2o**, 115591-40-7; **2p**, 74702-43-5; **3a**, 2769-64-4; **3a** (homopolymer), 28391-59-5; **3b**, 115591-41-8; **3b** (homopolymer), 115591-43-0; **3c**, 7188-38-7; **3c** (homopolymer), 28513-62-4; **3d**, 13947-76-7; **3d** (homopolymer), 106926-90-3; **3e**, 6697-95-6; **3e** (homopolymer), 114487-72-8; **3f**, 1195-99-9; **3f** (homopolymer), 114487-73-9; **3h**, 104876-31-5; **3h** (homopolymer), 115591-46-3; **3i**, 10340-91-7; **3i** (homopolymer), 60406-17-9; **3j**, 931-54-4; **3j** (homopolymer), 28390-20-7; **3k**, 10349-38-9; **3k** (homopolymer), 28390-21-8; **3g**, 2008-61-9; **3l**, 1930-89-8; **3l** (homopolymer), 115591-44-1; **3m**, 7050-85-3; **3m** (homopolymer), 115591-48-5; **3n**, 3128-77-6; **3n** (homopolymer), 115591-47-4; **3o**, 115603-32-2; **3p**, 115591-42-9; **3p** (homopolymer), 115591-45-2; (*S*)-(+)-C₂H₅CH(CH₃)NH₂, 513-49-5; (*S*)-(-)-C₆H₅CH(CH₃)NH₂, 2627-86-3; (*R*)-(+)-C₆H₅CH(CH₃)NH₂, 3886-69-9; (*S*)-(-)-*c*-C₆H₁₁CH(CH₃)NH₂, 17430-98-7; (*S*)-(-)-1-naphthylethylamine, 10420-89-0; (L)-(-)-ephedrine, 299-42-3; (*R,R*)-1,2-diaminocyclohexane, 20439-47-8; (L)-isoleucine methyl ester, 2666-93-5; (L)-prolinol, 23356-96-9; (L)-phenylalaninol, 3182-95-4; (L)-valine methyl ester, 4070-48-8; (L)-alanine methyl ester, 10065-72-2; (L)-cysteine methyl ester, 2485-62-3; 2-phenyl-2-bromopropane, 3575-19-7; α,α-dimethylbenzyl alcohol, 617-94-7; tetrakis(*tert*-butyl isocyanide)nickel(II) perchlorate, 40667-87-6; tetrakis(*tert*-pentyl isocyanide)nickel(II) perchlorate, 106859-37-4; tetrakis(2-*tert*-butylphenyl isocyanide)nickel(II) perchlorate, 115603-69-5; tetrakis(2,6-diisopropylphenyl isocyanide)nickel(II) perchlorate, 115650-89-0; tris(*tert*-butyl isocyanide)[(*S*)-(-)-(1-phenylethyl)amino-(*tert*-butylamino)carbene]nickel(II) perchlorate, 115603-71-9; tris(*tert*-pentyl isocyanide)[(*S*)-(-)-(1-phenylethyl)amino(*tert*-pentylamino)-carbene]nickel(II) perchlorate, 115603-73-1.

"Hydrophobic" Binding of Water-Soluble Guests by High-Symmetry, Chiral Hosts. An Electron-Rich Receptor Site with a General Affinity for Quaternary Ammonium Compounds and Electron-Deficient π Systems

Michael A. Petti,† **Timothy J. Shepodd,‡** **Richard E. Barrans, Jr., and Dennis A. Dougherty***

Contribution No. 7742 from the Arnold and Mabel Beckman Laboratories of Chemical Synthesis, 164-30, California Institute of Technology, Pasadena, California 91125.
Received February 22, 1988

Abstract: Several members of a new class of water-soluble macrocycles with well-defined, hydrophobic binding sites have been prepared and their binding properties analyzed. These hosts are built up from ethenoanthracene units and exist in meso (*C₂ₕ*) and *d,l* (*D₂*) forms. The latter have been synthesized enantiomerically pure, the key step being a highly selective asymmetric Diels-Alder reaction. Several of these hosts display a strong and fairly general affinity for quaternary ammonium compounds. We ascribe this effect to an ion-dipole attraction between the positively charged guests and the electron-rich π systems of the hosts. In addition, neutral guests with electron-deficient π systems are preferentially bound, suggesting the operation of favorable host-guest, donor-acceptor π-stacking interactions. Preliminary studies with chiral guests reveal some enantiospecific binding, with preferences as large as 3:1 observed.

Host-guest chemistry continues to develop as a major sub-discipline of modern chemistry.[1] The pioneering studies on crown ethers and related structures laid the foundations for the field.

They established that when appropriate amounts of preorganization[2] and complementarity between host and guest are designed

---

†Present address: Rohm & Haas, Springhouse, PA 19477.
‡Present address: Sandia National Laboratories, Livermore, CA 94551.

(1) For a general introduction to the host-guest field, see: *Top. Curr. Chem.* **1981**, *98*; **1982**, *101*; **1983**, *113*; **1984**, *125*; **1986**, *132*.
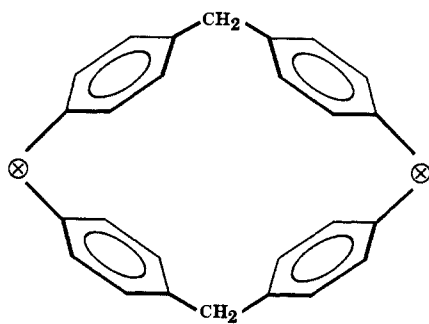
Figure 1. Basic Koga macrocycle. The structure that crystallized with durene encapsulated in the cavity had the linker, ⊗, equal to $-^+NH_2-(CH_2)_4NH_2^+$.

Scheme I

into synthetic macrocycles, quite efficient, selective hosts for a variety of inorganic and organic ions can be prepared.

It is perhaps a more challenging task to recognize and bind organic molecules in general, as the attractive forces involved are less well understood. Early advances in binding "organic" substrates focused on cyclodextrins.[3] These toroidal oligomers of glucose provide hydrophobic binding sites for a variety of relatively small organic molecules. Many elegant studies have established that these binding sites can be elaborated into catalysts that mimic enzymes in form and function.

Over the past decade it has become clear that in order to realize the full potential of this field, one must be able to rationally design and build hosts with hydrophobic binding sites. In this way, guests unable to fit into a cyclodextrin can be bound, and the often severe challenge of selective functionalization of the binding site can be more easily addressed. Early work[4] focused on large cyclophanes, and a variety of studies using somewhat indirect techniques indicated that hydrophobic binding was feasible with such molecules.

In 1980, Koga reported an X-ray crystal structure of a complex between durene as guest and a macrocyclic cyclophane host (Figure 1).[5a] The durene was completely surrounded by a hydrophobic cavity formed by the cyclophane. This critical observation provided the first direct evidence that such cyclophanes do indeed bind by encapsulation and, from our perspective, constituted a true turning point for the field. The many previous studies, and the even greater number to follow, were to a considerable extent validated by the Koga crystal structure.

In recent years, there has been considerable further development of water-soluble cyclophanes with hydrophobic binding sites,[5-10]
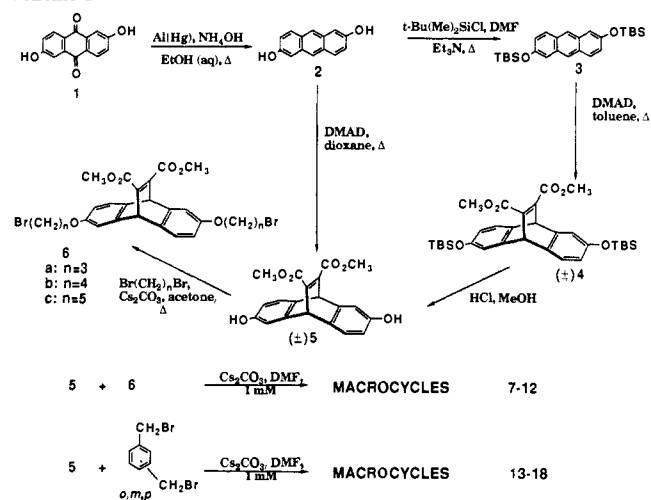
with the dominant theme being modification of the Koga macrocycle (Figure 1). The most easily transformed region is the "linker", ⊗, and several workers have varied this unit. Koga varied the length of the linker $[(CH_2)_n]$ and its rigidity.[5b] Lehn[7] and Koga[5c] introduced chirality by using tartrate-derived linkers, and Vögtle[8a] built an entirely carbocyclic host with carboxylates as solubilizing units. Diederich first introduced spiropiperidinium units emanating from the diphenylmethane carbon in an effort to remove the charge from the binding region. Later modifications by Diederich included the introduction of further spiropiperidinium units and methyl groups on the aromatic rings.[9a] Further development continues, and other designs have also received considerable attention.[10]

Design of a New Class of Hydrophobic Binding Sites. Several years ago we set out to develop a new class of water-soluble molecules with hydrophobic binding sites. Our initial goal, too, was to start with the Koga system—a structure known to bind organic molecules—and modify it in several important ways to enhance binding and the potential utility of the structures for applications in catalysis, transport, etc. The specific improvements we sought were as follows.

(2) Cram, D. J. *Angew. Chem., Int. Ed. Engl.* **1986**, *25*, 1039–1134.

(3) (a) Bender, M. L.; Komiyama, M. *Cyclodextrin Chemistry*; Springer-Verlag: Berlin, 1978. (b) Saenger, W. *Angew. Chem., Int. Ed. Engl.* **1980**, *19*, 344–362.

(4) Stetter, H.; Roos, E. *Chem. Ber.* **1955**, *88*, 1390–1395. Tabushi, I.; Kuroda, Y.; Kimura, Y. *Tetrahedron Lett.* **1976**, *37*, 3327–3330. Tabushi, I.; Sasaki, H.; Kuroda, Y. *J. Am. Chem. Soc.* **1976**, *98*, 5727–5728. Tabushi, I.; Kimura, Y.; Yamamura, K. *J. Am. Chem. Soc.* **1978**, *100*, 1304–1306. Tabushi, I.; Kimura, Y.; Yamamura, K. *J. Am. Chem. Soc.* **1981**, *103*, 6486–6492.

(5) (a) Odashima, K.; Itai, A.; Iitaka, Y.; Koga, K. *J. A. Chem. Soc.* **1980**, *102*, 2504–2505. (b) Odashima, K.; Soga, T.; Koga, K. *Tetrahedron Lett.* **1981**, *22*, 5311–5314. (c) Odashima, K.; Itai, A.; Iitaka, Y.; Arata, Y.; Koga, K. *Tetrahedron Lett.* **1980**, *21*, 4347–4350. (d) Soga, T.; Odashima, K.; Koga, K. *Tetrahedron Lett.* **1980**, *21*, 4351–4354. (e) Takahashi, I.; Odashima, K.; Koga, K. *Tetrahedron Lett.* **1984**, *25*, 973–976.

(6) Excellent reviews of this general area have appeared: (a) Franke, J.; Vögtle, F. *Top. Curr. Chem.* **1986**, *132*, 135–170. (b) Tabushi, I.; Yamamura, K. *Top. Curr. Chem.* **1983**, *113*, 145–183.

(7) Dhaenens, M.; Lacombe, L.; Lehn, J. M.; Vigneron, J. P. *J. Chem. Soc., Chem. Commun.* **1984**, 1097–1099.

(8) (a) Vögtle, F.; Merz, T.; Wirtz, H. *Angew. Chem., Int. Ed. Engl.* **1985**, *24*, 221–222. (b) Merz, T.; Wirtz, H.; Vögtle, F. *Angew. Chem., Int. Ed. Engl.* **1986**, *25*, 567–569. (c) Vögtle, F.; Müller, W. M. *Angew. Chem., Int. Ed. Engl.* **1984**, *23*, 712–714. (d) Franke, J.; Vögtle, F. *Angew. Chem., Int. Ed. Engl.* **1985**, *24*, 219–220. (e) Schrage, H.; Franke, J.; Vögtle, F.; Steckhan, E. *Angew. Chem., Int. Ed. Engl.* **1986**, *25*, 336–338. (f) Vögtle, F.; Müller, W. M.; Werner, U.; Losensky, H.-W. *Angew. Chem., Int. Ed. Engl.* **1987**, *26*, 901–903.

(9) (a) Diederich, F.; Dick, K. *Tetrahedron Lett.* **1982**, *23*, 3167–3170. (b) Diederich, F.; Dick, K. *Angew. Chem., Int. Ed. Engl.* **1983**, *22*, 715–716. (c) Diederich, F.; Dick, K. *J. Am. Chem. Soc.* **1984**, *106*, 8024–8036. (d) Diederich, F.; Griebel, D. *J. Am. Chem. Soc.* **1984**, *106*, 8037–8046. (e) Diederich, F.; Dick, K.; Griebel, D. *Chem. Ber.* **1985**, *11*, 3588–3619. (f) Kreiger, C.; Diederich, F. *Chem. Ber.* **1985**, *118*, 3620–3621. (g) Diederich, F.; Dick, K. *Chem. Ber.* **1985**, *118*, 3817–3829. (h) Rubin, Y.; Dick, K.; Diederich, F.; Georgiadis, T. M. *J. Org. Chem.* **1986**, *51*, 3270–3278. (i) Dharanipragada, R.; Diederich, F. *Tetrahedron Lett.* **1987**, *22*, 2443–2446. (j) Ferguson, S. B.; Diederich, F. *Angew. Chem., Int. Ed. Engl.* **1986**, *25*, 1127–1129. See also: Jazwinski, J.; Blacker, A. J.; Lehn, J.-M.; Cesario, M.; Guilhem, J.; Pascard, C. *Tetrahedron Lett.* **1987**, *28*, 6057–6060. Dharanipragada, R.; Ferguson, S. B.; Diederich, F. *J. Am. Chem. Soc.* **1988**, *110*, 1679–1690.

(10) Jarvi, E. T.; Whitlock, H. W. *J. Am. Chem. Soc.* **1982**, *104*, 7196–7204. Breslow, R.; Czarnik, A. W.; Lauer, M.; Leppkes, R.; Winkler, J.; Zimmerman, S. *J. Am. Chem. Soc.* **1986**, *108*, 1969–1979. O'Krongly, D.; Denmeade, S. R.; Chiang, M. Y.; Breslow, R. *J. Am. Chem. Soc.* **1985**, *107*, 5544–5545. Gutsche, C. D. *Acc. Chem. Res.* **1983**, *16*, 161–170. Canceill, J.; Lacombe, L.; Collet, A. *J. Am. Chem. Soc.* **1985**, *107*, 6993–6996. Canceill, J.; Lacombe, L.; Collet, A. *J. Chem. Soc., Chem. Commun.* **1987**, 219–221. Schneider, H.-J.; Philippi, K.; Pöhlmann, J. *Angew. Chem., Int. Ed. Engl.* **1984**, *23*, 908–909. Murakami, Y.; Kikuchi, J.-l.; Suzuki, M.; Takaki, T. *Chem. Lett.* **1984**, 2139–2142. Tobe, Y.; Fujita, H.; Wakaki, I.; Terashima, K.; Kobiro, K.; Kakiuchi, K.; Odaira, Y. *J. Chem. Soc., Perkin Trans. 1* **1984**, 2681–2684. Saigo, K.; Lin, R.-J.; Kubo, M.; Youda, A.; Hasegawa, M. *J. Am. Chem. Soc.* **1986**, *108*, 1996–2000. Hamilton, A. D.; Kazanjian, P. *Tetrahedron Lett.* **1985**, *26*, 5735–5738. Wilcox, C. S.; Cowart, M. D. *Tetrahedron Lett.* **1986**, *27*, 5563–5566. Wilcox, C. S.; Greer, L. M.; Lynch, V. *J. Am. Chem. Soc.* **1987**, *109*, 1865–1867. An alternative approach to molecular recognition involves hosts that are organic soluble. Binding is achieved primarily through hydrogen bonding, although some π-stacking may also be involved. See, for example: Rebek, J., Jr. *Science (Washington, D.C.)* **1987**, *235*, 1478–1484. Rebek, J., Jr.; Askew, B.; Ballester, P.; Buhr, C.; Jones, S.; Nemeth, D.; Williams, K. *J. Am. Chem. Soc.* **1987**, *109*, 5033–5035. Hamilton, A. D.; van Engen, D. *J. Am. Chem. Soc.* **1987**, *109*, 5035–5036.

Binding of Water-Soluble Guests by Chiral Hosts

*J. Am. Chem. Soc., Vol. 110, No. 20, 1988* 6827

(1) We sought a rigorous separation of the charged (hydrophilic) groups and the hydrophobic cavity. In the Koga prototype (Figure 1), water solubility requires protonation of the amines, making the charged moieties an intrinsic part of the "hydrophobic" cavity. We assumed that separating these two structural domains would increase the binding site's overall hydrophobicity and thus its binding ability. Concurrent with our efforts, Diederich described the important hosts mentioned above. While Diederich's design change did remove the charge from the macrocycle, the system was flexible enough that the charge could reach around into the binding region and directly interact with oppositely charged guests.[9a]

(2) The Koga system was soluble only at pH <2, and we sought to expand the solubility range to less severe environments. Other workers have also achieved this goal, primarily through the use of quaternary alkylammonium compounds[9,10] and carboxylates.[7,8a]

(3) The crown ether work and other studies firmly established that preorganization is critical.[2] The polymethylene chain of Koga's host is flexible, and he showed that more rigid linkers produced better hosts.[5b] In addition, though, the diphenylmethane propellers are quite flexible,[11] and so we sought to replace them by more rigid structures. Also, for catalyst development, one must be able to place functional groups at precise positions around the periphery of the binding site. Again the flexibility of the diphenylmethane unit hampers such efforts.

(4) Chirality is, of course, a desirable feature that would allow enantiospecific binding and, more importantly, asymmetric induction in catalysis. We sought a design that would produce an "inherently chiral"[12] binding site. That is, rather than designing a sphere or a cube and then perturbing it with one or more stereogenic centers ("chirally perturbed, inherently achiral binding site"[12]), we sought a design in which chirality was a natural feature of the entire structure. We anticipated that the "degree of chirality"[13] of such an intrinsically chiral receptor would be greater than that of a chirally perturbed receptor.

After considering many systems, we realized that a structure built up from a 2,6-disubstituted 9,10-ethenoanthracene would satisfy the above criteria. As shown in Scheme I, our basic building block arises from a Diels–Alder reaction[14] between dimethyl acetylenedicarboxylate and 2,6-dihydroxyanthracene.[15] This structure (5) contains many desirable features,[16] the first of which is an absolutely rigid, concave, hydrophobic surface. This locks the aryl rings into the "face-to-face" orientation known to be favorable for binding.[5a,6,9] Connecting two such structures (Figure 2) produces an array of four aromatic rings that must be a viable binding site, based on Koga's molecules and derivatives. The ester groups can, at any time, be converted to carboxylates, which then provide water solubility at near-neutral pH. The rigid ethenoanthracene also maintains the positions of the carboxylates in a region that is necessarily external to the binding site. Phenols were chosen as the means to introduce the linker ⊗. Our experience,[17] and that of others, indicated that phenols are especially well-suited to the remarkable Cs_2CO_3/DMF macrocyclization reagent.[18] Functional group placement should be straightforward in this system, since our building block is derived from an anthracene (and ultimately an anthraquinone). Organic chemists are quite capable of selective functionalization of anthracenes,

Figure 2. Meso and *d,l* macrocycles.
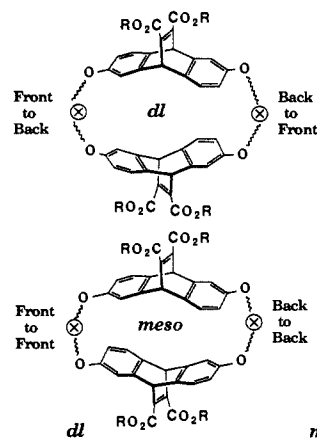
⊗	*dl*		*meso*	
	R = CH₃	R = Cs	R = CH₃	R = Cs
(CH₂)₃	7	III_dl	8	III_meso
(CH₂)₄	9	IV_dl	10	IV_meso
(CH₂)₅	11	V_dl	12	V_meso
[structure]	13	O_dl	14	O_meso
[structure]	15	M_dl	16	M_meso
[structure]	17	P_dl	18	P_meso
[structure]	19	C_l		

especially considering the many recent studies of the synthesis of anthracycline antibiotics.[19]

The final issue is chirality. Our bridged anthracene building block (5) has C_2 symmetry. It is chiral, but not asymmetric (dissymmetric). Whenever one dimerizes a chiral unit, two diastereomers are possible (Figure 2). Coupling opposite enantiomers, the heterochiral[20] coupling, produces a meso compound, which has C_{2h} symmetry in the present case. The homochiral[20] coupling produces the chiral, *d,l* diastereomer. This structure possesses three perpendicular, 2-fold axes and has D_2 symmetry. The difference between the two diastereomers can be seen in Figure 2. In the achiral isomer, the linkers run "front-to-front" and "back-to-back," producing a mirror plane perpendicular to the original 2-fold axis. In the chiral diastereomer, the linkers run "front-to-back" and "back-to-front," which imparts a sense of twist to the molecule. This host contains a helical cavity that is the inherently chiral binding site we seek. The value of 2-fold symmetry in chiral catalysts has been amply demonstrated by many structures based on binaphthyls and tartrates.[21] An additional advantage of this design is that when the ethenoanthracene building block is obtained enantiomerically pure, macrocyclization produces only one enantiomer of the chiral diastereomer. Thus, after a single resolution, a whole array of chiral hosts varying in the linker position ⊗ can be prepared.

In the present work we describe our initial studies of these structures. They are indeed easily prepared, freely water-soluble, and effective receptors for a variety of guests. Furthermore, we have prepared enantiomerically pure hosts and observed initial indications of enantiospecific binding.

(11) Barnes, J. C.; Paton, J. D.; Damewood, J. R., Jr.; Mislow, K. *J. Org. Chem.* **1981**, *46*, 4975–4979, and references therein.

(12) This terminology arises by analogy to similar descriptions of optically active chromophores. See, for example: Mislow, K. *Introduction to Stereochemistry*; W. A. Benjamin: Menlo Park, CA, 1965; pp 64–67.

(13) For a discussion of "fuzzifications" of the term chirality, see: Mislow, K.; Bickart, P. *Isr. J. Chem.* **1976/77**, *15*, 1–6.

(14) Sauer, J.; Wiest, H.; Mielert, A. *Chem. Ber.* **1964**, *97*, 3183–3207.

(15) (a) Goodall, F. L.; Perkin, A. G. *J. Chem. Soc.* **1923**, 470–476. (b) Hall, J.; Perkin, A. G. *J. Chem. Soc.* **1923**, 2029–2037.

(16) Petti, M. A.; Shepodd, T. J.; Dougherty, D. A. *Tetrahedron Lett.* **1986**, *27*, 807–810.

(17) Chang, M. H.; Masek, B. B.; Dougherty, D. A. *J. Am. Chem. Soc.* **1985**, *107*, 1124–1133.

(18) van Keulen, B.; Kellogg, R. M.; Piepers, O. *J. Chem. Soc., Chem. Commun.* **1979**, 285–286. Dijkstra, G.; Kruizinga, W. H.; Kellogg, R. M. *J. Org. Chem.* **1987**, *52*, 4230–4234.

(19) See, for example: Beak, P.; Snieckus, V. *Acc. Chem. Res.* **1982**, *15*, 306–311. For other lead references, see: Kelly, T. R.; Vaya, J.; Ananthasubramanian, L. *J. Am. Chem. Soc.* **1980**, *102*, 5983–5984. 2,6-Diamino-, dihydroxy-(anthraflavic acid), and disulfonylanthraquinone are commerically available. For the preparation of several other 2,6-disubstituted anthraquinones, see: Josephy, E.; Radt, F. *Elsevier Encyclopedia of Organic Chemistry*; Elsevier: New York, 1946; Vol. 13, Series III.

(20) Anet, F. A. L.; Miura, S. S.; Siegel, J.; Mislow, K. *J. Am. Chem. Soc.* **1983**, *105*, 1419–1426.

(21) Kagan, H. In *Asymmetric Synthesis*; Morrison, J. D., Ed.; Academic: New York, 1985; Vol. 5, Chapter 1. Finn, M. G.; Sharpless, K. B. *Ibid.* pp 247–308. Halpern, J. *Ibid.* pp 41–69. Takaya, H.; Ohta, T.; Sayo, N. Kumobayashi, H.; Akutagawa, S.; Inoue, S.; Kasahara, I.; Noyori, R. *J. Am. Chem. Soc.* **1987**, *109*, 1596–1597. Noyori, R.; Ohkuma, T.; Kitamura, M.; Takaya, H.; Sayo, N.; Kumobayashi, H.; Akutagawa, S. *Ibid.* **1987**, *109*, 5856–5858. Cram, D. J.; Cram, J. M. *Acc. Chem. Res.* **1978**, *11*, 8–14.

Table I. Macrocyclization Yields

macrocycles	yield, %	macrocycles	yield, %
7 + 8	35	15 + 16	36
9 + 10	51	17 + 18	18
11 + 12	40	19ᵃ	5.5
13 + 14	24		

ᵃ *trans*-1,4-Dimethylenecyclohexane ditosylate and (–)-5 were used in the macrocyclization reaction; all others used ±5 and the appropriate dibromide.

Not surprisingly, these hosts tightly bind highly water-insoluble guests such as anthracene and pyrene.[16] Such guests have a strong driving force to find an alternative environment to water, and a variety of organic macrocycles will bind them strongly. In the present work, we emphasize water-soluble guests. These molecules must make a choice between water and the environment provided by the host. True attractions between host and guest are involved, rather than repulsion between the guest and water. Using this approach, we have uncovered several new effects that can lead to tight, oriented binding of guests in well-defined, synthetic receptor sites.

Synthesis and Physical Characterization. Our synthetic approach is shown in Scheme I. Reduction of commercially available anthraflavic acid (1) provides 2,6-dihydroxyanthracene, (2).[15] Diphenol 2 undergoes a Diels–Alder reaction with dimethyl acetylenedicarboxylate (DMAD)[14] in refluxing dioxane over 48 h to give the racemic, C_2-symmetric ethenoanthracene building block 5 in 60% yield. The low yield reflects the ease with which DMAD undergoes Michael addition reactions. Protection of the phenols as *tert*-butyldimethylsilyl ethers eliminates the Michael addition problem and increases the diene solubility, allowing the reaction to be run in toluene. This improves the three-step (2–5) yield to 66% while providing the starting material 3 for our synthesis of enantiomerically pure 5 (see below). Diol 5 is alkylated in acetone with an excess of an α,ω-dibromide and Cs_2CO_3 as a base, producing the dibromides 6a–c in 55–70% yield.

Macrocyclizations are conducted in two different manners. For the polymethylene-linked macrocycles, dibromides 6a–c are cyclized with diol 5. For the xylyl- and cyclohexyldimethylene-linked macrocycles, 2 equiv of 5 are cyclized with 2 equiv of the desired xylylene dibromide or cyclohexyldimethylene ditosylate. All closure reactions are conducted in DMF using Cs_2CO_3 as a base[18] and employ high-dilution (1 mM) or syringe pump techniques. The yields (Table I) of the macrocycles, (7–19; Figure 2) are quite good, relative to the 1–10% yields more typically seen in this field. The relative ease with which these 26- to 32-membered rings are formed reflects the efficacy of the Cs_2CO_3/DMF reagent and the preorganized, concave shape of the precursors 5 and 6.

When the basic building blocks (5 and 6) are racemic, coupling them together yields equal amounts of the two previously discussed diastereomers (Figure 2), with the chiral diastereomer being racemic. In addition, all macrocyclizations produce higher molecular weight oligomers. The meso and *d,l* macrocyclic "dimers" are separated from higher molecular weight material by simple flash chromatography. Separation of the two diastereomeric tetraesters is achieved by preparative high-performance liquid chromatography. In all cases, the isomers are free from higher molecular weight material. Vapor-phase osmometry, ¹H NMR, ¹³C NMR, and mass spectral data (EI, FAB) indicate the structures to be the desired dimers.

With the macrocycles in hand, only the last step, the unmasking of the water-solubilizing functionality, remains. In our standard hydrolysis procedure, excess cesium hydroxide in DMSO/water cleaves the methyl esters. The reaction mixture is passed over a cation-exchange resin (NH_4^+ form), lyophilized, neutralized with CsOD, and dissolved in buffer to produce stock solutions of hosts used for binding studies.

Chiral recognition studies and asymmetric catalysis require enantiomerically pure hosts. An advantage of our scheme is that a whole array of such structures can be readily prepared once the basic building block 5 is obtained enantiomerically pure. After several unsuccessful attempts at a classical resolution,[22] we syn-
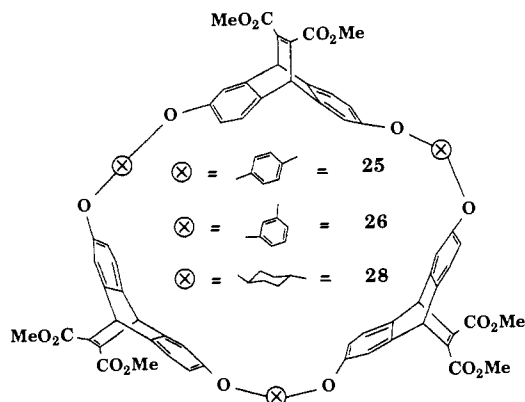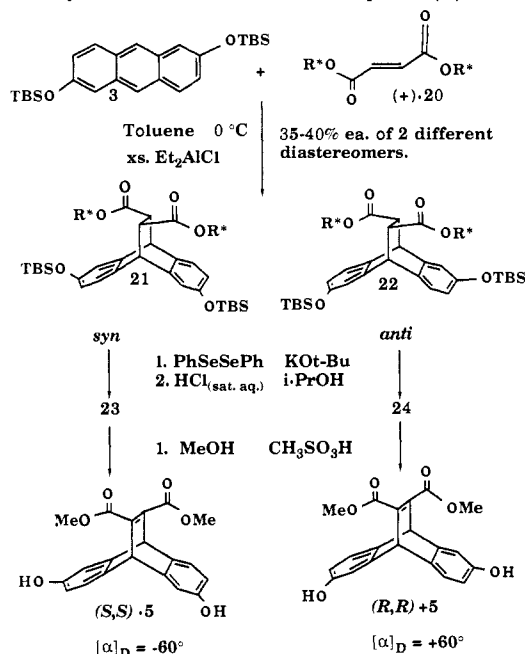

Figure 3. Trimer macrocycle structures. Analogous tetramer structures are 27 (*m*-xylyl-linked) and 29 (*trans*-1,4-dimethylenecyclohexyl-linked).

Scheme II. Asymmetric Diels–Alder Reaction [R* = (+)-menthyl]

thesized enantiomerically pure 5 directly utilizing an asymmetric Diels–Alder reaction.[23] The diethylaluminum chloride catalyzed[24] Diels–Alder addition of (+)-dimenthylfumarate (+20) to 3 (Scheme II) yields two of four possible diastereomers. All four isomers are produced in the uncatalyzed reaction. Complete facial selectivity at the dienophile[23,24] produces one syn (21) and one anti adduct (22). Compounds 21 and 22 are trivially separated by crystallization and separately elaborated to the two enantiomers of 5. The bridge double bond is introduced by using diphenyl diselenide with *tert*-butoxide. Deprotection of the phenolic silyl ethers followed by transesterification yields (–)-5 from 21 and (+)-5 from 22 (Scheme II).

A correct syn/anti assignment for the 21/22 pair is essential, because this assignment, along with the known olefin facial selectivity of the asymmetric Diels–Alder reaction,[23,24] determines the absolute configuration of 5. The assignment was made on the basis of several observations. The first was a two-dimensional, ¹H–¹H, NOE-correlated NMR (NOESY) study. Different bridge-to-aromatic cross peaks observed in the NOESY spectra for 21 and 22 allow the structural assignment. Second, the ¹H

(22) Many classical resolutions were attempted with a variety of chiral derivatives of 5, including resolutions of acids with alkaloid bases and crystallographic separation of diastereomeric imide and ether derivatives. These procedures are tedious and give low yields of partially enriched materials.

(23) Paquette, L. A. In *Asymmetric Synthesis*; Morrison, J. D., Ed.; Academic: New York, 1984; Vol. 3, Part B, Chapter 7.

(24) Furuta, K.; Iwanaga, K.; Yamamoto, H. *Tetrahedron Lett.* **1986**, *27*, 4507–4510.

Table II. Optical Rotations of Macrocycles and Host Structures

abs config[a]	compd	$[\alpha]_D$, deg	concn,[b] g/100 mL
S	(−)-5	−60	0.76
S	(+)-17	+144	1.1
S	(+)-25	+18	0.40
S	(+)-15	+58	1.0
S	(−)-26	−20	0.40
S	P_d	+358	0.058
S	M_d	+37	0.036
R	(+)-5	+61	0.23
R	(−)-17	−144	1.7
R	(−)-15	−51	3.2
R	(+)-26	+19	1.7
R	(+)-27	+65	1.0
R	(−)-19	−44	0.12
R	(−)-28	−8.4	0.15
R	(+)-29	+28	0.08
R	P_l	−364	0.021
R	M_l	−37	0.051
R	C_l	−133	0.037

[a]Absolute configuration of the ethenoanthracene building block in these structures. [b]Host rotations were measured in borate-*d* buffer, all others in acetonitrile.
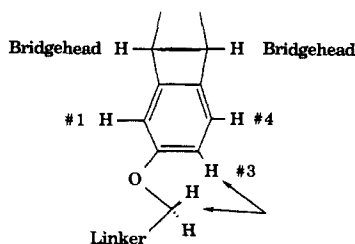

Figure 4. Schematic of the conformation around the O–CH₂ linkage of **17**. The close contact is indicated by the arrows.

NMR chemical shift patterns of **21** and **22** match qualitatively with the patterns observed for similar syn/anti pairs reported in the literature.[25] Further support for the assignment of absolute configuration comes from studies on a variety of C_2-symmetric bridged anthracenes, which show a consistent relationship between the sign of $[\alpha_D]$ and absolute configuration.[25] The rotations observed for **5** corroborate the **21/22** assignments.

An additional advantage of the use of enantiomerically pure **5** is the ease of isolation of pure samples of D_3-symmetric "trimers" **25, 26,** and **28** (Figure 3) and D_4-symmetric "tetramers" **27** and **29** (Figure 3). These are quite novel structures that certainly merit further investigation.

One interesting feature of the enantiomerically pure macrocycles (**15, 17, 19**) is their optical rotations. As Table II clearly indicates, the macrocycles have rotations quite different from their precursor building blocks. The tightly coiled, D_2-symmetric, dimer macrocycles have an intrinsically dissymmetric chromophore, which counteracts the intrinsic rotation of the bicyclic subunit. The larger macrocycles become more flexible and lose this conformationally enforced sense of twist, thus reverting toward the optical rotation of the bis(phenol) subunit. These observations support our argument that the dimers have helical, intrinsically chiral binding sites.

Good evidence exists for a strong conformational preference in tetraester **17**. In particular, intramolecular, ¹H NMR, difference NOE experiments in CD₂Cl₂ suggest that a single conformation at the aryl OCH₂ group predominates (Figure 4). Irradiation of the 3,7-protons of **17** (see Figure 5 for numbering) results in an enhancement of only one proton of the OCH₂ group and an enhancement at the 4,8-proton. Irradiation of the 1,5-protons, under identical conditions, results in an enhancement of only the bridgehead protons. This suggests that only one of the OCH₂ protons is proximate to the 3,7-protons and that neither of the OCH₂ protons is near the 1,5-position. The idealized
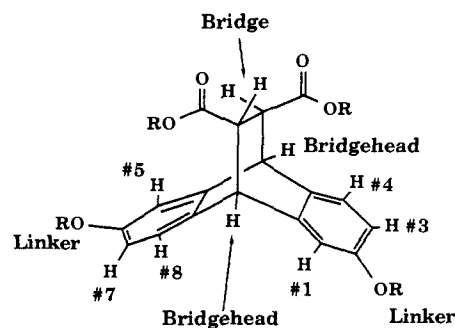

Figure 5. Numbering scheme for Diels–Alder adducts and macrocycles. The name of each proton is placed next to its position.

geometry about the aryl OCH₂ groups shown in Figure 4 is consistent with this result. For the cyclohexyl-linked macrocycle **19**, the same NOE enhancements are observed, while the polymethylene-linked macrocycles fail to give any compelling NOE results. For all the macrocycles, both esters in organic solvents and carboxylates in water, the NMR spectra indicate high-symmetry structures. Attempts to detect any dynamic process by low-temperature NMR experiments have been unsuccessful.

CMC Studies. Our hosts, like those of other workers, are structurally similar to surfactants, having both hydrophobic and hydrophilic parts. At sufficiently high concentrations, the molecules aggregate. Without a knowledge of the state of aggregation of such hosts, interpretations involving specific 1:1 host–guest interaction should be viewed with caution. In all our binding studies we work at concentrations below those at which significant host aggregation occurs. We use NMR to evaluate the aggregation behavior of our hosts and determine what we loosely refer to as a critical micellar concentration (CMC).[26] All our CMC's are on the order of 0.2–0.8 mM.

One point that must also be considered is the aggregation of host structures in the presence of guest molecules. Certainly, the addition of guest has an influence upon the aggregation of host, as one can imagine that a host–guest complex could be more hydrophobic than the host alone. Specific and consistent NMR shift patterns of the guest upon binding to a host provide strong evidence against such aggregation,[6] and in the vast majority of the cases studied herein, aggregation of the host–guest complex does not appear to be a problem. However, we do have some evidence for aggregate-type binding behavior (see section on ATMA).

Binding Studies. Determination of Binding Affinities from NMR Shift Data. All binding affinities reported herein were obtained from ¹H NMR studies. All spectra of a guest in the presence of a host show only time-averaged signals of complexed and uncomplexed guest. Assignment of the association constant is made from a best fit between the observed positions of the guest resonances at varying host and guest concentrations and the resonances predicted from our complexation model. The unknowns are the association constant (K_a) and the upfield shift of fully complexed guest relative to that for free guest, which we will call D. The quality of the fit is determined in the least-squares sense, with the optimal parameters (K_a and D) chosen as those yielding the smallest sum of squares of the residuals (differences between observed and predicted NMR resonances).

As the model for the guest NMR resonances is not linear in the association constant, an iterative rather than an analytical means for optimizing the parameters is required. A single association constant and the upfield shift for each guest proton are obtained from the NMR data by a Levenberg–Marquardt procedure[27] (MULTIFIT). The NMR data from all guest protons are simultaneously fit with a single association constant. This nec-

(25) Hagishita, S.; Kuriama, K. *Tetrahedron* **1972**, *28*, 1435–1467.

(26) (a) Fendler, E. J.; Constien, V. G.; Fendler, J. H. *J. Phys. Chem.* **1975**, *79*, 917–926. (b) Mukerjee, P.; Mysels, K. J. *J. Natl. Stand. Ref. Data Ser., Natl. Bur. Stand.*, **1971**, *No. 36.*

(27) Press, W. H.; Flannery, D. P.; Teukolsky, S. A.; Vetterling, W. T. *Numerical Recipes: the Art of Scientific Computing*; Cambridge University: New York, 1986; pp 521–525.

6830   *J. Am. Chem. Soc., Vol. 110, No. 20, 1988*

Petti et al.

essarily produces the most reliable association constant, in a least-squares sense, corresponding to the entire data set. This approach is superior to employing the simple average of several association constants obtained from fitting to individual protons, both because the true least-squares value is obtained and because the resultant regression has more degrees of freedom. An NMR experiment in which m different spectra (reflecting different host and guest concentrations) are recorded on a guest molecule with n protons will involve a total of $N = n \times m$ observations. Under MULTIFIT, there are $n + 1$ parameters to be optimized: the single association constant and the D values of each of the n guest protons. When protons are fitted individually, there are two parameters to be fitted for each. Since the number of degrees of freedom of a regression is equal to the number of observations minus the number of fitted parameters, the MULTIFIT regression has $N - n - 1$ degrees of freedom, while an independent regression of each proton has a total of $N - 2n$. Our model assumes 1:1 binding, and the quality of the regression fits supports this approach. In addition, we have simulated shift patterns that would result from 1:2 and 2:1 binding, and we find that our systems in general are not compatible with such models.

Conspicuously absent from most previous studies of binding by NMR has been any discussion of the error bars one should place on the binding affinities obtained. This is a complex problem, and we have investigated several aspects of it. A complete analysis of the valid confidence limits of these fitting procedures is in progress and will be described separately. We can at this point, though, make several relevant observations. We have first attempted to address the different uncertainties in the various measurements using a weighted least-squares, nonlinear regression program (EMUL) we have developed. This program seeks to minimize, rather than the simple sum of squares of the residuals, the corresponding sum in which each residual is weighted inversely by the estimated uncertainty in the corresponding observation,

$$X^2 = \sum_{i=1}^{N} \frac{(\delta_{obsd} - \delta_{pred})^2}{\sigma_i^2}$$

The estimated variance σ_i^2 is calculated as the sum of the contributions from each of l independent random variables x, according to the formula[28]

$$\sigma^2_{\delta_{obsd}} \approx \sum_{l=1}^{l} \sigma^2_{x_l} \left(\frac{\partial x_l}{\partial \delta_{obsd}} \right)^2$$

The seven random variables $x_1, ..., x_7$ considered are (1) observed chemical shift in the sample, (2) chemical shift of uncomplexed guest, (3) concentration of host stock solution, (4) concentration of guest stock solution, volumes of (5) host and (6) guest stock solutions, and (7) volume of buffer in the sample. The standard deviations σ_{x_l} are assigned values based on reasonable expectations of the possible systematic errors as well as random uncertainties in the various measurement techniques. We find that no one variable has an especially large influence on the results and that the optimized parameters determined by EMUL do not differ significantly from those derived from MULTIFIT.

Our current estimate of the error bars on our binding affinities derives from observations on the reproducibility of the data and from simulations that demonstrate the range of results that give satisfactory fits to the data. We feel that a realistic error bar for $\Delta G°_{295K}$ is $\pm$ 200 cal/mol. Note that, in this case, only association constants that differ by a *factor of 2* can be considered as meaningfully different. We believe that error bars of this magnitude are relevant to all determinations of association constants by NMR under rapid-exchange conditions.

Control Experiments with "Half-Molecule". We believe that specific and sizeable upfield shifts of guest protons provide strong evidence for binding by encapsulation in the host cavity. Strong support for such conclusions can be obtained from binding studies with a structure that is closely related to the hosts, but that lacks

Chart I
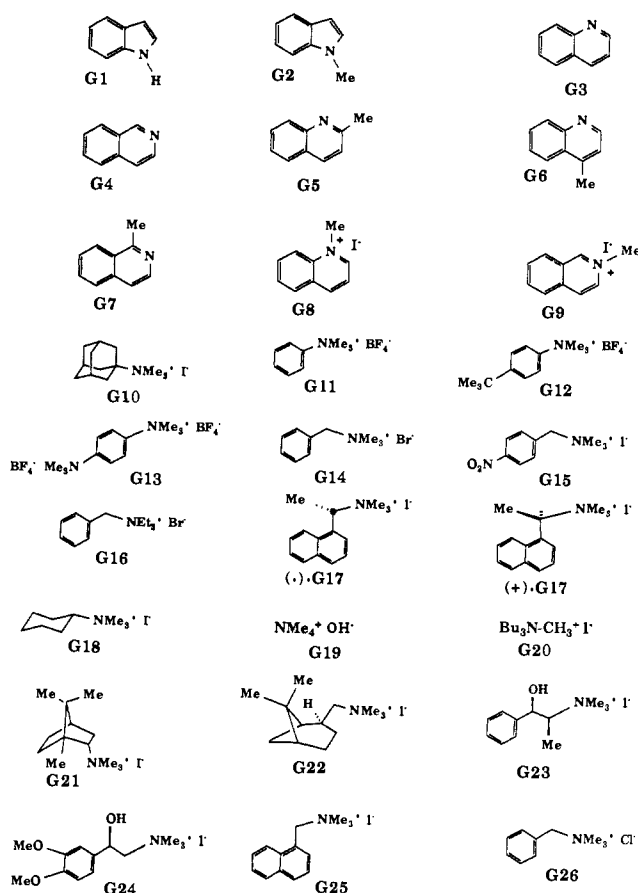
Table III. Binding Affinities for Aromatic Heterocyclic Guests[a]

guests	hosts				
	V_{dl}	C_l^b	P_d^c	M_l^c	sol[d]
G1	e	4.3	4.2	e	0.016
G2	e	4.8	4.5	4.4	0.0032
G3	3.9	5.9	5.4	4.6	0.078
G4	4.3	6.3	6.3	4.6	0.037
G5	3.5	5.8	5.5	4.5	0.023
G6	4.0	6.0	6.2	4.5	0.014
G7	4.2	6.7	6.4	4.5	0.030
G8	5.3	6.3	7.6	6.7	0.52
G9	5.1	6.0	7.2	6.6	0.45

[a] All values represent $-\Delta G°_{295}$ (kcal/mol) in borate-d buffer. Values accurate to ± 0.2 kcal/mol. [b] R,R,R,R absolute configuration. [c] Both enantiomers of host were used in these studies. [d] Guest solubility (M), as determined in borate-d buffer. [e] Insignificant upfield shifts of guest protons were observed in these experiments.

the macrocyclic cavity. In the present system, we use the "half-molecule"[16]—the dicesium salt of the diethyl ether of **5 (31)**. In all cases, only trivial NMR shifts are seen when guests are added to solutions of this structure. Comparable shifts are seen in the presence of cesium maleate.

Flat, Aromatic Guests. Donor–Acceptor π-Stacking and Ion–Dipole Effects. In an effort to evaluate electronic features that may aid molecular recognition, we have studied a series of similarly sized and shaped, water-soluble guests with differing electronic properties.[29] Flat aromatic guests G1–G9 (Chart I) bind to several of our hosts with moderate to exceptionally strong affinities (Table III). P_d and C_l bind all of these guests in the same conformation, as indicated by consistent and specific ^1H NMR chemical shift changes that occur upon binding. All protons of

---

(28) Bevington, P. R. *Data Reduction and Error Analysis for the Physical Sciences*; McGraw-Hill: New York, 1969; p 60.

(29) A preliminary report on some aspects of this work has appeared: Shepodd, T. J.; Petti, M. A.; Dougherty, D. A. *J. Am. Chem. Soc.* **1988**, *110*, 1983–1985.
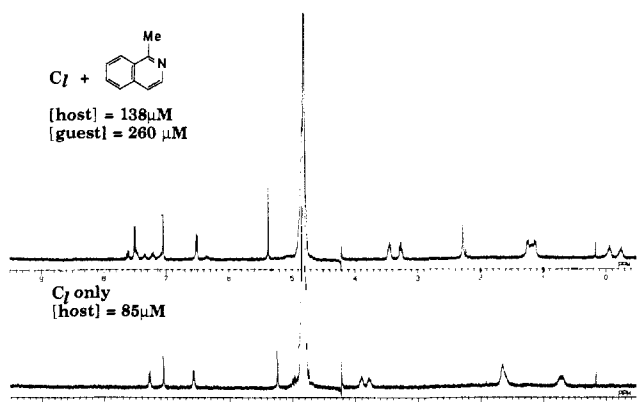
Binding of Water-Soluble Guests by Chiral Hosts

J. Am. Chem. Soc., Vol. 110, No. 20, 1988 6831

Figure 6. Host–guest binding experiment: borate-*d* buffer, pD ≈ 9.
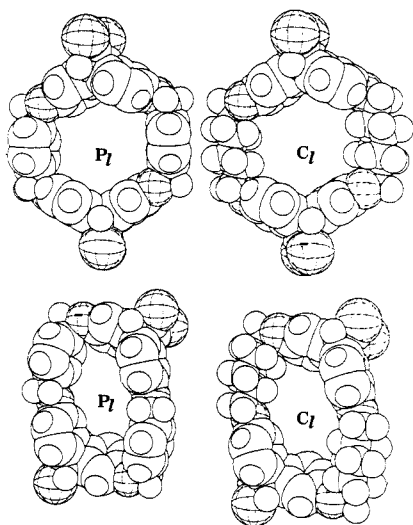

Figure 7. Space-filling schematics of P and C in the toroid (top) and rhomboid (bottom) conformations. Oxygens in the macrocycle are hatched, and the carboxylates are truncated to hatched spheres for clarity.

the guests move upfield; the protons of the hosts also show specific changes upon binding. For C$_l$ with flat, aromatic guests, large upfield shifts of all linker protons are observed, as shown in Figure 6 for the guest 1-methylisoquinoline. In addition, the 4,8-protons (Figure 5) of the host move downfield. For P$_d$, several protons move upfield; the 1,5-, 3,7-, OCH$_2$, and linker protons all experience shielding upon binding flat aromatic guests. The 4,8-protons shift downfield. All of these shifts indicate that both P and C preferentially bind these guests in C$_2$-symmetric rhomboid conformations (Figure 7).[30] Unlike the toroidal, D$_2$ conformation (Figure 7, see below), the two openings of the cavity are inequivalent in the rhomboid conformation. Chemical shifts changes of the host suggest the guest is displaced toward the back opening, as displayed in Figure 7.

The rhomboid cavity is ideally suited to naphthalene-sized guests, in that they fit snugly within the cavity without excess space. This situation maximizes hydrophobic binding by occluding water molecules from the hydrophobic environment of the receptor site. We see this with the electron-rich[31] indole (G1) and 1-methylindole (G2) guests. No strong donor–acceptor (D/A) interactions should exist between the host and guest, since both

are electron-rich. The driving force for binding should result mostly from van der Waals attractions between the sparsely soluble indoles and the encapsulating host, as well as from the free energy gain associated with expelling the highly organized water surrounding the free host and guest.

The rhomboid conformation binds the other flat aromatic guests (G3–G9) with much higher affinities. The quinolines and isoquinolines are quite similar in size and shape to the indoles, and so the enhanced binding is not a consequence of increased steric complementarity. The rhomboid conformation is well suited for π-stacking interactions with flat aromatic guests. The electron-rich aromatic rings of P and C can lie directly above the below the plane of the bound guest, and we attribute the enhanced binding to strong π-stacking D/A interactions between the electron-rich hosts and the electron-deficient[31] quinoline and isoquinoline guests. Apparently, the anisole rings of the ethenoanthracene units dominate the π-stacking, since P and C have similar binding affinities for guests G1–G7. These additional D/A attractions are worth at least 1 kcal/mol in binding affinity (Table III). The actual D/A stabilization is probably greater, because the quinolines and isoquinolines are more water-soluble than the indoles (Table III), and thus should experience a reduced hydrophobic attraction.

Methylation of quinoline and isoquinoline affords the very water-soluble *N*-methylquinolinium and *N*-methylisoquinolinium. On a per gram basis, these compounds are more water-soluble than salts such as sodium bicarbonate and sodium phosphate.[32] Yet, they are very strongly bound by our hydrophobic receptors. We would expect that alkylation would further enhance donor–acceptor interactions, and this appears to be the case. The hydrophilicity of these guests should significantly reduce the driving force for association with a hydrophobic binding site, and so the similar binding affinities of cationic guests G8, G9 toward C$_l$ (Table III) relative to their neutral counterparts G3, G4 indicate a substantial enhancement in attractive host–guest interactions.

P$_d$ binds these charged guests (G8, G9) much more tightly than C$_l$ (Table III). Studies with the "isostructural" guest pairs (G5/G9, G7/G8, G6/G8) indicate that this is not a steric or hydrophobic effect. These are very large binding constants for such freely soluble guests—the $-\Delta G°_{295}$ of 7.6 kcal/mol for P/G8 corresponds to a K_a of over 400 000 M^{-1}. We attribute the enhanced binding of these cationic guests to a polarization of P$_d$ in response to the positive charge of the guest. This ion–dipole effect is significant and can be worth more than 1 kcal/mol in binding free energy.

This charge effect is not a direct electrostatic effect of the type observed by other workers.[5,7-9] When charged groups on a host come into close contact with complementary charges on a guest, enhanced binding affinities are observed. In our systems, however, the rigid macrocyclic framework prevents the carboxylates from coming into close contact with the positively charged guests. The NMR shift patterns clearly show that the guest is encapsulated in the central cavity of the host. It is difficult to envision a set of host contortions that could place the carboxylates near the positive charge of the bound guest. More importantly, if P could somehow achieve such a geometry, host C, which is very similar in structure, could also. However, only P, with its fully aromatic binding site, shows the enhanced ion–dipole effect.

Additional support for the operation of an ion–dipole effect is seen in host M. Only two values for binding affinities are seen within our error bars. The neutral, aromatic guests show a moderate attraction ($-\Delta G°_{295} ≈ 4.5$ kcal/mol), and the charged quinolinium and isoquinolinium guests show an exceptional attraction ($-\Delta G°_{295} ≈ 6.5$ kcal/mol). Models show that M can adopt many different binding conformations, so we cannot confidently ascribe a precise orientation to the guest in the binding site. However, the host NMR shift patterns observed upon binding are the same for all the guests, suggesting a common binding conformation. The extra strong binding affinities for the charged, flat guests is a measure of the strength of the ion–dipole effect.

(30) Structures in Figures 7 and 13 are intended to convey approximate dimensions only. They are, in fact, the results of full geometry optimizations on the appropriate structures, minus the carboxyl groups on the etheno bridges. The force field used was a modified (to include more realistic aryl ether parameters) version of the Dreiding molecular mechanics field found in the program BIOGRAF (Biodesign, Inc., Pasadena, CA). Since this is a relatively simple force field, and since the calcutions refer to isolated molecules in the gas phase, we consider the results to be only qualitative.

(31) Joule, J. A.; Smith, G. F. *Heterocyclic Chemistry*, 2nd ed. Van Nostrand Reinhold: London, 1978.

(32) *CRC Handbook of Chemistry and Physics*; Weast, R. C., Ed.; CRC: Cleveland, OH, 1974.
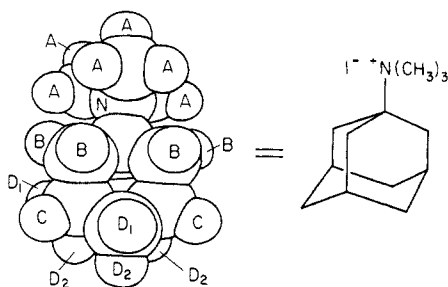
6832 J. Am. Chem. Soc., Vol. 110, No. 20, 1988

Petti et al.

Figure 8. ATMA (G10) with labels for each type of guest proton.

While this is to our knowledge the first demonstration of the importance of such ion–dipole effects in synthetic receptors of this sort, these types of interactions are well-documented, in gas-phase ion studies[33] and protein crystal structures.[34]

These studies on water-soluble, aromatic guests show that true "molecular recognition" can be achieved in such systems. The difference in binding affinity between N-methylindole and N-methylquinolinium is 3 kcal/mol with host P, and this is a lower limit (remembering water solubility) for the combined effects of D/A and ion–dipole interactions.

Adamantyltrimethylammonium (ATMA). Our initial CPK model-building studies emphasized the toroid conformation shown in Figure 7[30] and indicated that our host cavity was of the proper size and shape to encapsulate an adamantyl compound. We chose the amine derivative adamantyltrimethylammonium iodide (G10; see Figure 8) because it is quite water-soluble, and its high symmetry (C_{3v}) made it amenable to low-concentration ^1H NMR studies.[35]

We expected that if ATMA were to bind within our host cavities, its protons should experience extensive shielding from the aromatic rings of the host. ATMA has five types of protons, labeled A, B, C, D_1, and D_2 in Figure 8, and the cylindrical shape of the molecule places these in unique positions relative to each other. The A protons and B protons each form a ring that is perpendicular to the C_3 axis of ATMA. Protons C and D_1, although they are different types, form a third cylindrical ring. However, the D_2 protons are in a quite different orientation and point roughly parallel to the C_3 axis of ATMA.

The idealized binding orientation for ATMA suggested by CPK models is one in which the C_3 axis is approximately parallel to the etheno bridges of the host. In such an orientation, ATMA protons A, B, and (C + D_1) would point out toward the aromatic rings of the host and should be substantially shielded. In contrast, the D_2 protons would point out toward the solvent and should experience less shielding. The relative ordering of the shielding of the protons within this idealized geometry will depend upon the depth of penetration of ATMA into the binding site.

We have observed three types of binding orientations for ATMA within the receptor site of our hosts. The first, typified by the tetramethylene-linked hosts, shows no discrimination in the shielding patterns among the ATMA protons (Table IV). We believe this is most likely a consequence of multiple binding orientations for the guest in what may be a shallow, hydrophobic cleft created by a collapse of the host out of the toroid conformation of Figure 7. The second binding orientation, typified by the m-xylyl-linked and the pentamethylene-linked hosts, shows a predominant association with the trimethylammonium (TMA) group, in that the A and B protons are the most highly shielded. Importantly, the significant shielding of D_2, equivalent in magnitude to the shielding of C and D_1, indicates that ATMA does not bind solely in the idealized geometry discussed above. As will be shown below, this TMA binding effect is fairly general. The third binding orientation, typified by P and C, is completely

Table IV: Binding of ATMA (G10) to Several Hosts

host	D_A	D_B	D_C	D_{D1}	D_{D2}	$-\Delta G°_{295}$[b]
			D values[a]			
IV_{meso}[c]	0.91	1.02	0.99	1.09	1.10	5.2
IV_{dl}[c]	0.75	0.65	0.60	0.80	0.90	4.2
V_{meso}[c]	2.51	2.84	0.96	1.10	0.97	4.6
V_{dl}[c]	2.44	2.80	1.43	1.52	1.33	4.4
P_{dl}[c]	1.85	2.90	1.19	1.30	0.76	6.9
C_l[d]	1.25	2.64	0.92	1.02	0.41	5.4
V_{dl}[d]	1.41	1.58	0.89	0.93	0.89	5.3
P_{dl}[d]	1.95	3.09	1.22	1.23	0.75	6.7
M_{dl}[d]	1.15	0.92	0.48	0.52	0.47	5.5

$^aD = \delta_G = \delta_{HG(satn)}$ in ppm; $D > 0$ indicates an upfield shift. ^{b}As determined by the MULTIFIT procedure. ^{c}In phosphate buffer, pD ≈ 7.5. ^{d}In borate-d buffer.
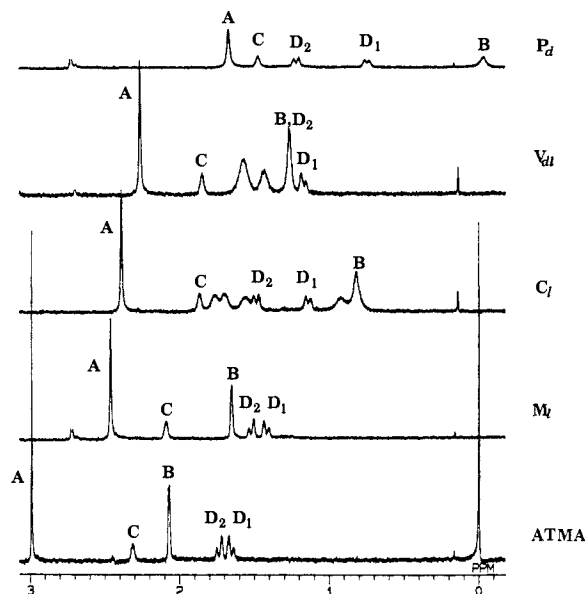

Figure 9. NMR studies of ATMA with various hosts $[H]_0 = [G]_0 = 150$ μM in borate-d. The peaks at 2.75 ppm (DMSO) are truncated for clarity; external reference at 0.00 ppm.

consistent with the binding of ATMA in the idealized geometry. For both hosts P and C, the A and B protons are both shielded, although A is significantly less shielded than in the TMA-binding mode described above. Most importantly, the shieldings of C and D_1 are comparable, while that of D_2 is substantially less, as we had anticipated.

The different binding modes—oriented (with hosts P_d and C_l) and nonoriented (with hosts M_l and V_{dl})—are clearly discernable from the respective ^1H NMR spectra of the host–guest complexes (see Figure 9). The Δv of the AB pattern clearly shows the crucial D_1–D_2 differentiation. For both P_d and C_l, a large Δv is observed, consistent with oriented binding. In contrast, for hosts M_l and V_{dl}, the pattern resembles the AB pattern of free ATMA. This requires similar shielding of both D_1 and D_2, indicative of the nonoriented binding mode.

The binding affinities (Table IV) reveal several interesting trends. Even the nonspecific binders show relatively large affinities, compared to those usually seen for an aliphatic guest.[36-38] However, host P_d shows a greatly enhanced affinity for ATMA. This is a very large binding affinity for a freely water-soluble, aliphatic guest. ATMA has a special affinity for our hosts as

(33) Meot-Ner (Mautner) M.; Deakyne, C. A. *J. Am. Chem. Soc.* **1985**, *107*, 469–474. Deakyne, C. A.; Meot-Ner (Mautner), M. *Ibid.* **1985**, *107*, 474–479.

(34) Burley, S. K.; Petsko, G. A. *FEBS Lett.* **1986**, *203*, 139–143.

(35) Shepodd, T. J.; Petti, M. A.; Dougherty, D. A. *J. Am. Chem. Soc.* **1986**, *19*, 6085–6087.

(36) See, for example: References 5b, 8c, and 9g.

(37) Cyclodextrins and their derivatives are also effective at binding adamantane derivatives. See, for example: (a) Emert, J.; Breslow, R. *J. Am. Chem. Soc.* **1975**, *97*, 670–672. (b) Tabushi, I.; Shimokawa, K.; Shimizu, N.; Shirakata, H.; Fujita, K. *J. Am. Chem. Soc.* **1976**, *98*, 7855–7856, and ref 38.

(38) Gelb, R. 1.; Schwartz, L. M.; Laufer, D. A. *J. Chem. Soc., Perkin Trans. 2* **1984**, 15–21. Cromwell, W. C.; Byström, K.; Eftink, M. R. *J. Phys. Chem.* **1985**, *89*, 326–332. Harrison, J. C.; Eftink, M. R. *Biopolymers* **1982**, *21*, 1153–1166.

Binding of Water-Soluble Guests by Chiral Hosts

J. Am. Chem. Soc., Vol. 110, No. 20, 1988 6833

compared to all the other TMA guests studied (see below). The adamantyl structure ties back the aliphatic skeleton slightly and may allow the charged TMA group better access to favorable ion–dipole interactions with our hosts. Also, the smooth cylindrical shape of ATMA fills complementary host cavities or clefts snugly, maximizing hydrophobic type binding. These features, plus its highly informative ^{1}H NMR parameters, should make ATMA a valuable guest for evaluating the binding abilities of various hosts.

In our preliminary report[35] on these systems, we noted the striking difference between V_{dl} and P_d, and we ascribed this to the greater preorganization of the more rigid host P. However, host C_l is equally preorganized, and binds ATMA in the idealized geometry, yet does not show an exceptionally high affinity. We now recognize that the special affinity of P_d for ATMA reflects ion–dipole attractions of the sort just described. The magnitude of the effect (P_d vs C_l) is quite comparable to that seen with quinolinium compounds (see above), and taken together these results indicate that host P constitutes a quite general binding site for quaternary ammonium compounds. The better comparison for evaluating the effects of preorganization is perhaps V vs C.[5b] This is certainly not a perfect pairing since a cyclohexyl is also "wider" and perhaps slightly longer than $(CH_2)_5$. With this caution, the comparison suggests that the dominant effect of preorganization is to produce more highly oriented binding.

The specific chemical shifts for each of the types of ATMA protons unambiguously demonstrate the ability of P_d to bind ATMA in an extremely specific orientation, but this is not the only type of binding that occurs. At higher concentrations, near or above the CMC of P_d, the pattern of chemical shift variations deviates from the specific pattern seen at lower concentrations. Instead, all the protons of ATMA show similar chemical shift changes with increasing percentage guest bound. This is completely consistent with nonspecific, aggregate-type binding, where the guests associate randomly among aggregates of host and host–guest complex.

We have measured the enthalpy and entropy of binding of ATMA to two of our hosts. For IV_{meso} $\Delta H° = -5 \pm 2$ kcal/mol and $\Delta S° = 0 \pm 3$ eu; for V_{meso} $\Delta H° = -3 \pm 2$ kcal/mol and $\Delta S° = 5 \pm 3$ eu (cesium phosphate buffer,[35] pD ≈ 9.5). Although the accuracy of these data is limited, the implications are clear. As with earlier studies involving adamantyl compounds binding to cyclodextrins,[38] our systems are displaying the "nonclassical hydrophobic effect".[39] This is what one would expect for a relatively water-soluble guest.

Other TMA-Substituted Guests. Subsequent to our study of ATMA, we set out to examine our hosts' abilities to bind other closely related guests. We found the trimethylammonium substituent to be an effective NMR probe as well as an easy, convenient way to introduce water solubility. We therefore studied a series of substituted trimethylammonium salts of the general formula $RN(CH_3)_3^+X^-$ (R-TMA). By varying the guest and host structure, such parameters as the shape and size of both components involved in the molecular recognition event can be examined. Furthermore, we hoped to assess other factors such as the effect of charge on the binding event. Table V displays the

Table V. Binding Affinities for TMA-Substituted Guests[a]

	hosts					
guests	V_{meso}	P_{meso}	V_{dl}	C_l^b	P_d^c	M_f^c
G10			5.3	5.4	6.7	5.5
G11		5.0	4.6			
G12		5.7	5.6			
G13		5.3	5.0			
G14	4.6	5.1	4.6	4.9		
G15	5.1	5.6	5.3	5.2		
G16	4.4	5.6				
(-)-G17	4.5	5.9				
G18	4.7	5.5	4.9	d		
G19	3.3			4.5	4.7	
G20			4.2	d	5.2	5.0
G25			5.7	5.6		
G26			4.5			

[a] All values represent $-\Delta G°_{295}$ (kcal/mol) in borate-d buffer. Values accurate to ± 0.2 kcal/mol. [b] R,R,R,R absolute configuration. [c] Both enantiomers of host were used to determine these numbers. [d] Insignificant upfield shifts of guest protons were observed in these experiments.

binding affinities found in these studies.

The TMA Effect. Preliminary studies quickly revealed that the trimethylammonium (TMA) substituent, which was originally chosen as a water-solubilizing group, is quite often directed into the interior of the macrocycles, rather than exposed to the aqueous environment. In fact, several of our hosts can be considered quite general receptors for TMA's. Although they are charged, quaternary ammonium compounds can be quite hydrophobic, as evidenced by their extensive use as phase-transfer catalysts. In addition, these structures can display strong ion–dipole attractions for our hosts.

In order to further evaluate the TMA effect, we studied the guests G11–G13 which are all simple, substituted benzenes. For both V_{dl} and P_{meso}, p-*tert*-butylphenyl-TMA (G12) binds more tightly than phenyl-TMA (G11). The addition of a *tert*-butyl group enhances the hydrophobicity of the guest and increases its binding affinity. The addition of a second TMA group [G11 vs phenyl-1,4-bis(TMA) (G13)] also led to an increased affinity. This effect is especially significant considering that the addition of a TMA group presumably greatly increases the water solubility of the guest.

Perhaps the most interesting comparison is between G12 and G13, in which a *tert*-butyl is converted to a TMA. Here, the issue of charge is being addressed. If the binding is governed by the charge, then the doubly charged G13 should be the stronger binder. If hydrophobicity is the dominant factor behind the observed trends in binding affinities, then the very water-soluble G13 should bind significantly less than G12. Both these molecules have the same shape and size; thus, the trends in the data cannot be ascribed to the different fits of these guests within the cavity of the hosts.

The results for both V_{dl} and P_{meso} are similar. Guest G12 is more strongly bound to these hosts relative to G8 (≈ 0.5 kcal mol). Thus, the electrostatic interaction of the negatively charged host and positively charged TMA is not the sole binding force, for if it were, the dication G13 would be the better guest. The fact that G13 is also more strongly bound than G11 (≈ 0.4 kcal/mol), despite the increase in water solubility, illustrates the strong general affinity of our hosts for TMA units. This can lead to strong binding of a very hydrophilic guest (G13), close in magnitude to the binding observed with the more hydrophobic guest G12.
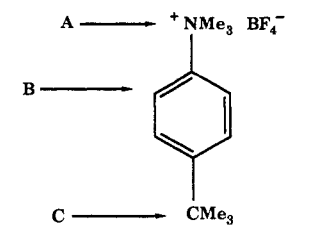
Interestingly, it is not necessarily the most hydrophobic group that is buried within the cavity of the host. In fact, for G12 and both hosts, the geometry of the host–guest complex is one where *the TMA end of the molecule is the most shielded* by the host. Therefore, when presented with a *tert*-butyl or a TMA group, these hosts prefer to place the less hydrophobic, charged group in the shielding region. Figure 10 shows the D values for the guest in these host–guest combinations. The larger D values for the TMA end of the molecule indicate that it resides deepest within the binding site of the host, in a region where any close contacts with the carboxylates would be impossible.

(39) Briefly, the classical hydrophobic effect displays a small, generally unfavorable $\Delta H°$, and a large, favorable $\Delta S°$. This is seen with highly insoluble solutes and is interpreted in terms of the usual water-structure arguments. In contrast, for more soluble guests, one can see a larger, favorable $\Delta H°$ and a small, often unfavorable $\Delta S°$. It is argued that release of water structure is less important for such guests and that true (enthalpic) attractions between host and guest dominate the binding. For a more extensive discussion of the present system, see: Petti, M. A. Ph.D. Thesis, California Institute of Technology, 1988. See also: Tanford, C. *The Hydrophobic Effect*, 2nd ed.; Wiley: New York, 1980. Jenks, W. P. *Catalysis in Chemistry and Enzymology*; McGraw-Hill: New York, 1969. References 3b and 36.

(40) Breslow, R. *Isr. J. Chem.* **1979**, *18*, 187–191.
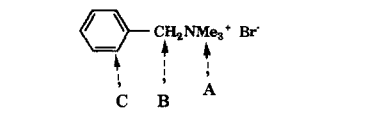
(41) We refer to borate-d loosely as a cesium borate buffer. Actually, aqueous borate chemistry is complex, and a number of different borate species are present. See: *Supplement to Mellor's Comprehensive Treatise on Inorganic and Theoretical Chemistry*; Longman: London, 1980; Vol. 5, pp 321–426.

(42) We thank Bryan Hamel and the scientific staff at the U.S. Borax Co. for advice about borate chemistry and for samples of high purity boric oxide.
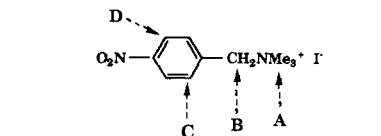
HOST	DA	DB	DC

Vdl | 1.40 | 2.10 | 0.30

Pmeso | 1.89 | 3.14 | 0.54

Figure 10. D values ($\delta_G - \delta_{HG(satn)}$) in ppm) for ($p$-$tert$-butylphenyl)trimethylammonium (G12) and the hosts V_{dl} and P_{meso}.

HOST	DA	DB	DC
Pmeso	2.24	3.01	2.60 (ortho)
Vmeso	1.40	2.04	1.47 (ortho)
Vdl	1.73	2.37	1.72 (ortho)
Cl	0.57	-----	2.70 (ortho)
			2.13 (meta)

HOST	DA	DB	DC	DD
Pmeso	1.53	2.20	2.54	1.70
Vmeso	0.45	0.94	1.90	2.57
Vdl	0.61	1.24	2.07	1.52
Cl	0.43	-----	2.26	2.32

Figure 11. D values ($\delta_G - \delta_{HG(satn)}$) in ppm) for benzyltrimethylammonium (G14) and (p-nitrobenzyl)trimethylammonium (G15) with various hosts.

The Nitro Effect. We have previously shown that hosts P and C preferentially bind electron-deficient quinoline systems relative to electron-rich indoles. Guests G14 and G15 provide a second opportunity to assess this effect. Figure 11 and Table V present further evidence for an electron-deficient group binding within the cavity of our hosts. p-Nitrobenzyl-TMA (G15) binds more strongly to all the hosts than does benzyl-TMA (G14). This undoubtedly reflects an enhanced donor–acceptor interaction. The electron-rich anisole-like aromatic rings of our host interact favorably with the electron-deficient nitroaromatic ring of the guest. This effect would appear to be worth ≈0.5 kcal/mol, although this analysis neglects differential guest solubility effects. Diederich[9j] has previously observed similar effects in methanol as solvent, but apparently not in water.

In addition to the increase of binding affinity upon the introduction of a nitro group, an interesting geometry change occurs upon binding. Figure 11 shows the D values for these complexes. While P_{meso} shows no strong preference for either end of the molecules, the other hosts place the nitro end of the guest within the cavity of the host. The effect is especially pronounced for C_l, and the aromatic ring of the benzyl guest (G14) is also recognized by this host in preference to the TMA group. This recognition of aromatic rings by C_l is general.

Table VI. Binding Affinities for Enantiomerically Pure Guests[a]

chiral guests	hosts			
	P$_l$[b]	P$_d$[c]	M$_l$[b]	M$_d$[c]
(+)-G17	5.8	6.3		
(−)-G17	6.7	5.9	4.7	4.2
G21	6.4	6.5	4.9	4.7
G22	5.1	4.5	5.1	4.7
G23	4.6	4.7	4.9	4.7
G24	5.8	5.7	5.1	4.7

[a] All values represent $-\Delta G°_{295}$ (kcal/mol) in borate-d buffer. Values accurate to ±0.2 kcal/mol. [b] R,R,R,R absolute configuration. [c] $S,S,$-S,S absolute configuration.

Linker Flexibility. The data for two meso hosts, V_{meso} and P_{meso}, with guests G14 and G16–G18 show some interesting trends (Table V). For V_{meso} all the guests bind with similar values. This suggests that perhaps the TMA group is predominantly responsible for the binding, although tetramethylammonium (G19) binds only weakly to V_{meso}. On the other hand, P_{meso} displays some selectivity, apparently discriminating among the guests by responding to increased hydrophobicity. Throughout Table V, in all direct comparisons of the polymethylene-linked macrocycles with the more rigid xylyl-linked macrocycles, the latter are always the more efficient hosts. This further illustrates[5b] the limitations of polymethylene spacers in this field and could reflect the effects of preorganization.[2] However, host C is certainly more rigid than V, but these two hosts show comparable binding abilities. Again, this suggests that the stronger binding by the xylyl-linked hosts is more a result of ion–dipole effects than preorganization.
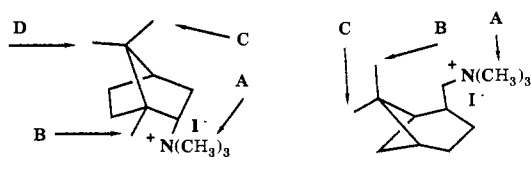
Guest Flexibility. We have also studied the effect of guest flexibility on the binding event. Our initial efforts emphasized a comparison between ATMA and tri-n-butylmethylammonium iodide (G20), both C$_{13}$ guests. As shown in Table V, ATMA always shows the stronger binding affinity, suggesting that guest flexibility plays a similarly detrimental role as does host flexibility. However, further studies with C$_{13}$ guests bornyl-TMA (G21) and myrtanyl-TMA (G22) (see below) indicate that the situation is more complex and host dependent.

Chiral Guests. Chiral Aliphatic Guests. Series of NMR binding experiments were performed with the chiral, aromatic-linked hosts (each enantiomer of M and P) and a series of chiral TMA guests [(+)-G17, (−)-G17, G21–G24; Chart I, Table VI]. We wished to see if our somewhat rigid hosts could discriminate between enantiomers of guests and bind them with substantially different free energies. The interactions between a single host enantiomer and opposite guest enantiomers are necessarily diastereomeric, but unless the energetic difference between diastereomeric complexes is substantial, the eventual usefulness of such systems is limited. We would like to design systems that can separate guest enantiomers; this requires strong, selective binding.

The bornyl-TMA (G21) and (cis) myrtanyl-TMA (G22) guests were chosen because of their similarity in size (all are C$_{13}$) and shape to ATMA. As ATMA has a strong binding affinity for M and P, we felt these two globular aliphatic TMA guests would similarly fill the hydrophobic receptor site and bring the TMA moiety into a favorable position for an ion–dipole interaction with the host. However, the only strong binding affinity is between P and bornyl-TMA. P with myrtanyl-TMA and M with both G21 and G22 show only moderate binding affinities that are not much larger than the control values for G19 as a guest.

As M does not bind ATMA fully enclosed within its receptor site, it also does not include similarly sized bornyl-TMA or myrtanyl-TMA. The D values (Figure 12) calculated for the complexes of bornyl-TMA and myrtanyl-TMA with M show that the TMA end of the guest experiences the largest upfield shifts as it complexes with the host, although the effect is small. The result is only moderate stabilization upon binding these two guests.

P_l and P_d both bind bornyl-TMA strongly. The D values indicate that some of the aliphatic protons of the guest are also pulled into the cavity of the host. The D value for the TMA is the largest for all the guest protons, yet the remainder of the molecule is also strongly associated with the host cavity. In

Binding of Water-Soluble Guests by Chiral Hosts

J. Am. Chem. Soc., Vol. 110, No. 20, 1988 6835

HOST	DA	DB	DC	DD	DA	DB	DC
P$_d$	1.44	1.01	0.74	0.57	1.97	0.92	0.34
P$_l$	1.27	0.90	0.61	0.52	2.47	1.36	0.48
M$_d$	0.61	0.42	0.32	0.33	0.62	0.16	0.13
M$_l$	0.78	0.58	0.46	0.43	0.86	0.28	0.24

Figure 12. D values ($\delta_G - \delta_{HG(satn)}$ in ppm) for G21 and G22 with the hosts P$_d$, P$_l$, M$_d$, and M$_l$.

contrast, when P binds myrtanyl-TMA, the TMA group is preferably complexed over the remainder of the guest. In myrtanyl-TMA the TMA group extends out farther from the main aliphatic skeleton than in bornyl-TMA. The stronger binding for bornyl-TMA might arise because of the proximity of the aliphatic skeleton to the TMA. This difference is small, but could cause the bornyl unit to be further encapsulated by the host as the TMA moves into an optimal position for ion–dipole attractions. The stronger affinity of P for ATMA supports this analysis, in that all of the aliphatic framework of ATMA is surrounded by the host.

Though P binds bornyl-TMA strongly, it shows no enantiospecificity. Interestingly, P binds myrtanyl-TMA less strongly, but with much greater enantiospecificity. The $\Delta\Delta G°$ of 0.6 kcal/mol is a substantial affinity difference. The 4.5 kcal/mol binding affinity for P$_d$ with myrtanyl-TMA shows that this association is equivalent to that of P$_d$ with G19, purely an attraction to the TMA group. The complex of P$_l$ with myrtanyl-TMA has an extra ≈ 0.5 kcal/mol in stabilization as compared to the complex P$_d$ with myrtanyl-TMA. The nature of this extra stabilization is not clear.

Chiral Aromatic Guests. We also studied chiral guest TMA's containing aromatic rings [(+)-G17, (−)-G17, G23, G24) (Table VI). For G17, both enantiomers of host and guest are available, providing two independent cross-checks of the data. P$_l$ and P$_d$ with (+)-G17 and (−)-G17 show measurable enantiospecificity in the binding affinities ($\Delta\Delta G° \approx 0.6$ kcal/mol).

Distinct and consistent chemical shift changes in both hosts (P$_d$ and P$_l$) and guests [(+)- and (−)-G17] indicate different binding orientations for the two diastereomeric complexes. For both complexes, the TMA portion of the guest is bound deepest within the receptor site; the naphthalene is at the edge of the cavity, only partially enveloped by the host. P binds the G17 guests in the toroid conformation, not in the rhomboid conformation. The host–guest pairs with the strong binding affinity (e.g., P$_l$ + (+)-G17) bind with the CCH$_3$ group placed into the cleft of the ethenoanthracene and the smaller methine hydrogen pointing into the xylyl linker (Figure 13).[30] The diastereomeric host–guest pairs (e.g., P$_l$ + (−)-G17) bind with the CCH$_3$ group pointing into the linker and the methine hydrogen pointing into the ethenoanthracene cleft (Figure 13). The weaker binding observed in the latter complex could be a consequence of an adverse steric interaction between the CCH$_3$ group and the host linker when the TMA is at its ideal position. While the enantiospecificity observed is small, it does suggest a model for further development, such that increasing the steric difference between the CH$_3$/H pair could increase $\Delta\Delta G°$.

Host P binds G23 more weakly than the naphthyl guests, but in the same host orientation. Again, the TMA is placed within the center of the idealized open conformation of the hosts and the aromatic ring sticks out into the water, but the net attraction is weaker and no enantiospecificity is seen. The presence of the alcohol hydroxyl could be the reason for the weaker association
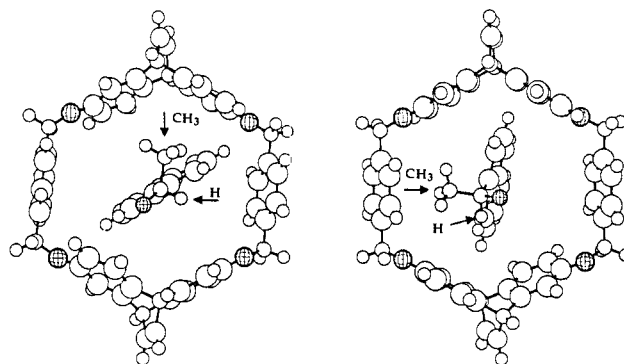

Figure 13. Ball and stick schematics of two possible binding conformations for host P$_l$ with (+)-G17 (left) and (−)-G17 (right). The benzylic methyls and hydrogens are indicated with arrows. The heteroatoms are hatched. The cesium carboxylates are truncated, and only the nitrogens of the TMA groups are shown.

experienced between P and G25. The solvated polar alcohol should prefer the aqueous environment and would be destabilized by the hydrophobic receptor environment.

P binds G24 with a strong binding affinity of 5.8 kcal/mol, but with no enantiospecificity. Interestingly, P binds the aromatic ring of G24 in the rhomboid conformation. Unlike all other TMA guests with P, the TMA group resides outside the cavity of the receptor. The trisubstituted benzene in G24 is roughly the size and shape of a naphthalene moiety and fits well within the cavity of rhomboid P. The dimethoxy-substituted ring of G24 is very electron-rich, so one might not expect strong stabilization when this ring sits within the six electron-rich rings of P. However, its presence within the cavity is preferred. Considering that even the electron-rich indoles G1 and G2 bind P with ~ 4.0 kcal/mol of binding energy, the result with G24 is reasonable. The hydrophobic aromatic ring binds within the hydrophobic host cavity; the water-soluble alcohol and TMA functionalities bind at the edge of the cavity, exposed to the water. The overall attraction is still strong at 5.8 kcal/mol.

In contrast to P, all of the chiral TMA guests, as well as G19, bind to M with the same affinity ($-\Delta G° = 4.7 \pm 0.2$), within experimental error. The one exception is the pair M$_d$ + (−)-G17 ($-\Delta G° = 4.2$ kcal/mol). These uniform moderate associations are attractions between the TMA of the guest and the polarizable aromatic rings of the host, combined with a slight hydrophobic attraction.

Summarizing the results of the studies of binding chiral guests, we see that our hosts show, at best, only moderate discrimination between the opposite enantiomers of asymmetric guests. Although NMR shift studies show that diastereomeric host–guest interactions always develop, thus far, both enantiomers of the host can find favorable binding orientations with these guests.

Discussion

At the outset of this work, we established a list of design criteria for a new class of water-soluble molecules with hydrophobic binding sites. The results described herein suggest that, to a considerable extent, the hosts of Figure 2 satisfy these standards. They are readily synthesized, water-soluble under mild conditions, and an efficient class of receptors for a variety of guests. From this first round of studies on these hosts, several interesting effects have been uncovered that could be of general interest in recognition and catalysis.

Perhaps the most remarkable feature of these molecules is their general, strong affinity for quaternary ammonium compounds. This is manifest with both trimethylammonium (TMA) and quinolinium-type guests and is especially pronounced when the "walls" of the host are completely aromatic as in P and M. We have attributed this effect to an ion–dipole attraction between the positive charge of the guest and the polarizable π bonds of the host.

Precisely such an effect has been observed in the gas phase both experimentally and theoretically.[33] Subsequently, Burley and

6836 *J. Am. Chem. Soc., Vol. 110, No. 20, 1988*

Petti et al.

Petsko[34] illustrated the biological significance of this interaction. A statistical analysis of 33 high-resolution protein crystal structures revealed a significant tendency for positively charged amino groups to lie in close contact to the π clouds of aromatic side chains. This interaction with the face of an aromatic ring contrasts the attraction of electron-rich moieties (oxygen, sulfur) to the electron-poor edge of such rings. Our results demonstrate that such ion-dipole interactions can greatly enhance binding in synthetic receptors. They also suggest the use of our hosts as catalysts for reactions that develop a positive charge in the transition state, and we are pursuing this line of reasoning.

Very recently[43] Stoddart and co-workers investigated a number of complexes between electron-rich, poly(ether) hosts and pyridinium guests, making extensive use of X-ray crystallography. They found a general tendency for the cationic nitrogen of the guest to lie collinearly between two ether oxygens, forming an electrostatically favorable $[O^{\delta-}\cdots N^{\delta+}\cdots O^{\delta-}]$ array. Our systems could also benefit from such interactions. However, as before, both P and C could experience such attractions, and so we consider it unlikely that these forces are primarily responsible for the strong affinity of P for quaternary ammonium compounds.[44]

An additional electronic effect, a π-donor/acceptor interaction, is evident in both the indole/quinoline and benzyl-/nitrobenzyl-TMA comparisons. Such effects are certainly not surprising, given the very electron-rich nature of the π systems of the ethenoanthracenes. They are, however, only minimally documented in the host/guest field. As mentioned above, Diederich's hosts show similar results in methanol as solvent, but no such effect could be observed in aqueous media.[9j]

Effects such as ion–dipole and donor–acceptor attractions, along with the previously mentioned close electrostatic contacts seen in other systems, constitute true "molecular recognition". They are superimposed upon a base-line hydrophobic effect, in which water-insoluble structures seek out nonpolar environments. While there is certainly some crude size and shape selectivity in strictly hydrophobic binding, the kind of tight, specific and oriented binding that one associates with biological receptors certainly requires these additional, more directed effects. In the present context, the magnitude of the various electronic effects is seen in a comparison such as N-methylindole (G2) vs N-methylquinolinium (G8). These molecules have very similar sizes and shapes and both fit very snugly into the rhomboid cavity. Yet the latter exhibits ca. 3 kcal/mol in enhanced attraction for P, even though it is much more water-soluble. This corresponds to a selectivity of almost 200:1. The ability of these effects to produce highly oriented binding is clearly demonstrated by the studies with ATMA.

An intriguing aspect of this work is the conformational behavior of the most rigid hosts, P and C. We designed these structures to contain a minimal amount of conformational flexibility, and our early studies with CPK models focused on the aesthetically appealing toroidal conformation. This perspective was enhanced by the observed tight, oriented binding of ATMA, a guest that fits snugly into the toroidal form. However, the binding of flat, aromatic guests (G1–G9) and the chemical shift changes involved

were inconsistent with the toroid form. Further CPK modeling studies revealed that the ether linkages can act as hinges, and the molecules can easily pivot between toroid and rhomboid forms. These hosts are two-state receptors, with a long, slender binding site that is complementary to flat aromatic systems and a broader, nearly circular form that accepts groups such as ATMA and other TMA compounds. It would, of course, be interesting to know whether both conformations also exist in the absence of guest, but we have been unable to obtain any data relevant to this point.

The situation is somewhat different in the polymethylene-linked hosts (III, IV, V). These molecules are relatively nonspecific binders, and there are no indications of strongly preferred binding orientations. To the contrary, the ATMA results strongly suggest that multiple binding orientations are involved. This appears to be detrimental to binding and would certainly be harmful to catalysis studies, where precise functional group positioning is essential. Our work thus provides further confirmation of the dictum "flexibility is the enemy".[40] Studies across the whole range of host–guest chemistry, including similar findings by Koga in his basic system[5b] (Figure 1), support this viewpoint.

Our basic host structures are intrinsically chiral and, because of the remarkable efficacy of the asymmetric Diels–Alder reaction,[23,24] are readily available in enantiomerically pure form. As observed by other workers,[5e,9b,9i] when a single enantiomer of a host is combined with opposite enantiomers of a chiral guest, one obtains diastereomeric complexes that are easily distinguishable by high-field NMR. *Such effects must occur and in no way indicate enantiospecificity*, i.e., the preferential binding of one particular enantiomer. To demonstrate enantiospecific binding one must independently determine the binding affinities of each enantiomer. Given the relatively large error bars on binding affinities as determined by NMR methods, only substantial enantiospecificities can be quantified. Since we estimate our error bars as ± 0.2 kcal/mol in $\Delta G°_{295}$, only if two values differ by more than 0.4 kcal/mol can the difference be considered meaningful. Of the several studies of chiral guests summarized in Table VI, many show absolutely no selectivity, but several indicate enantiospecificities that are at or above the 0.4 kcal/mol limit. The most promising case is the P/G17 pair. There are four measured $\Delta\Delta G°_{295}$ values, and they average to 0.65 kcal/mol. This implies a 3:1 selectivity. In addition, specific chemical shift patterns suggest the model summarized in Figure 13, which can serve as a starting point for the development of host–guest combinations that are more likely to produce high enantiospecificities.

Experimental Section

Uncorrected melting points were recorded on a Thomas-Hoover melting point apparatus. NMR spectra were recorded on Varian EM-390, XL-200, JEOL JNM GX-400, or Bruker WM-500 spectrometers. *J* coupling is reported in hertz. Routine spectra were referenced to the residual proton and carbon signals of the solvents and are reported (ppm) downfield of 0.0 as δ values. Binding event spectra were referenced to external TSP (0.00 ppm) in a coaxial tube. Infrared and ultraviolet spectra were recorded on a Perkin-Elmer 1310 infrared spectrometer and a Hewlett-Packard 8451 diode array ultraviolet spectrometer, respectively. Optical rotations were recorded on a Jasco DIP-181 digital polarimeter at 295 $\pm$ 2 K. HPLC and reverse-phase HPLC (RPHPLC) were performed on a Perkin-Elmer Series 2 liquid chromatograph. Preparative HPLC used a 1 in. $\times$ 25 cm Vydac 101HS1022 silica column, RPHPLC used a 2.0 $\times$ 25 cm Whatman Partisil M20 10/25 OD5-3 C_{18} column. Chromatographic eluents are reported as volume-to-volume ratios (v/v).

Solvents were distilled from drying agents: methylene chloride, CaH_2; toluene, sodium metal; ethereal solvents, sodium benzophenone ketyl. Dimethylformamide (DMF) was distilled at room temperature from calcined CaO and stored over at least two successive batches of activated 4-Å sieves. All reactions were stirred magnetically under inert atmospheres unless otherwise mentioned.

Host and guest stock solutions for the NMR binding experiments were made up with a standard 10 mM deuteriated cesium borate buffer at pH $\approx$ 9 (referred to as borate-*d*).[41] The buffer was made by dissolving 31.3 mg of high purity boric oxide[42] in 100 g of D_2O, adding 467 μL of 1 M CsOD in D_2O, and mixing thoroughly. All volumetric measurements of these solutions were made with adjustable volumetric pipets. The concentrations of the solutions were quantified by NMR integrations against

(43) Allwood, B. L.; Colquhoun, H. M.; Doughty, S. M.; Kohnke, F. H.; Slawin, A. M. Z.; Stoddart, J. F.; Williams, D. J.; Zarzycki, R. *J. Chem. Soc., Chem. Commun.* **1987**, 1054–1057. Allwood, B. L.; Shahriari-Zavareh, H.; Stoddart, J. F.; Williams, D. J. *J. Chem. Soc., Chem. Commun.* **1987**, 1058–1061. Allwood, B. L.; Spencer, N.; Shahriari-Zavareh, H.; Stoddart, J. F.; Williams, D. J. *J. Chem. Soc., Chem. Commun.* **1987**, 1061–1064. Allwood, B. L.; Spencer, N.; Shahriari-Zavareh, H.; Stoddart, J. F.; Williams, D. J. *J. Chem. Soc., Chem. Commun.* **1987**, 1064–1066. Ashton, P. R.; Slawin, A. M. Z.; Spencer, N.; Stoddart, J. F.; Williams, D. J. *J. Chem. Soc., Chem. Commun.* **1987**, 1066–1069.

(44) Another possible origin of the affinity of these hosts for cationic guests is a long-range electrostatic attraction between the positive charge of the guest and the carboxylates. A bound guest is surrounded by a medium of lower dielectric constant than water, so longer range Coulombic attractions could be important. Although this is likely a contributing factor, it does not explain the differences between P and C. Also, more recent work from our laboratories demonstrates strong binding of cationic guests by the uncharged, tetraester 17 in $CHCl_3$: D. A. Stauffer and D. A. Dougherty, unpublished results.

a primary standard solution of known concentration. All pulse delays for the integration experiments were at least 5 times the measured T_1 for the species involved. All binding studies were performed at 400 MHz.

2,6-Dihydroxyanthracene (2). 2,6-Dihydroxyanthracene was prepared by a modification of the procedure of Perkin.[15] Anthraflavic acid (50 g, 0.20 mol, 1 equiv), ethanol (400 mL), water (900 mL), and ammonium hydroxide (200 mL, saturated aqueous) were placed in a 3-L flask fitted with a thermometer. Aluminum amalgam, made from granular Al (109 g, 4 mol, 20 equiv) dipped in 1.5% aqueous mercuric chloride for 30 s, was added to the reaction in several portions and the reaction slowly heated to 60–65 °C. Vigorous stirring was maintained throughout the reaction. *Caution!* The reaction can get out of control; higher temperatures lead to overreduction with the 9,10-dihydroanthracene derivative being formed. The reaction temperature was maintained by intermittent use of a water bath. After 2 h, the yellow slurry was cooled to 0 °C and decanted away from the amalgam onto 1 L of ice stirring with 200 mL of 37% HCl. Any excess acid was destroyed with NaHCO₃ (to pH 4–5), and the entire reaction was frozen solid and then lyophilized. The lyophilized brown solid was slurried with three 1-L portions of acetone and filtered through a Celite pad. Yellow **2** (green fluorescent) in the filtrate was isolated by evaporating the acetone. Compound **2** was stored in the dark at <0 °C: yield, 33 g (78%); ¹H NMR (acetone-d_6) δ 7.28 (dd, 2 H, J = 7.5, 1.5), 7.38 (d, 2 H, J = 1.5), 7.98 (d, 2 H, J = 7.5), 8.28 (s, 2 H), 8.68 (s, 2 H, exchangeable with D₂O); ¹³C NMR (acetone-d_6) δ 154.58, 132.29, 130.18, 124.23, 120.98, 107.92. Compound **2** can be crystallized from ethanol: mp 294–297 °C (lit.[32] 295–300 °C).

2,6-Bis(*tert*-butyldimethylsiloxy)anthracene (3). 2,6-Dihydroxyanthracene (10.0 g, 0.048 mol, 1 equiv) and *tert*-butyldimethylsilyl chloride (21.5 g, 0.142 mol, 3 equiv) were dissolved with stirring in 500 mL of DMF under argon. Triethylamine (14.4 g, 0.142 mol, 3 equiv) was added, and the reaction turned black immediately. The reaction was stirred at 35 °C for 8 h and cooled to room temperature. The DMF was removed under vacuum yielding 40 g of an orange-black semisolid that was suspended in 100 mL of petroleum ether/ether (9/1), placed on a 100-g flash silica pad, and eluted with more solvent. The yellow (blue fluorescent) band was collected and evaporated yielding **3**, which is 95% pure. Pure material was obtained by recrystallizing the anthracene from hot petroleum ether (35–60 °C), yielding 17.5 g of yellow plates (83%): mp 123–125 °C; ¹H NMR (CDCl₃) δ 8.17 (s, 2 H), 7.82 (d, 2 H, J = 8), 7.25 (d, 2 H, J = 2), 7.07 (dd, 2 H, J = 2, 8), 1.02 (s, 18 H), 0.26 (s, 12 H); ¹³C NMR (CDCl₃) δ 151.82, 131.26, 128.98, 128.60, 123.93, 123.17, 113.21, 26.04, 18.56, –3.88; EI-MS; *m/e* 438 (M⁺), 381 (M – *t*-Bu); HRMS 438.2425, calcd for C₂₆H₃₈O₂Si₂ 438.2410.

2,6-Bis(*tert*-butyldimethylsiloxy)-9,10-dihydro-11,12-dicarbomethoxyethenoanthracene (4). A 25-mL round-bottomed flask was charged with **3** (1.35 g, 3.02 mmol, 1 equiv), 3 mL of freshly distilled toluene, and 1.9 mL of DMAD (2.19 g, 15.4 mmol, 5 equiv). The solution was refluxed for 42 h and then concentrated. MeOH (20 mL) was added, and the solution was sonicated to induce crystal formation; first crop 805 mg. The mother liquors were chromatographed on silica gel using 20% Et₂O/petroleum ether as an eluant giving 720 mg of a white solid: mp 123–126 °C (total yield 1.53 g, 86%); ¹H NMR (CDCl₃) δ 7.05 (d, 2 H, J = 8.1), 6.75 (d, 2 H, J = 2.2), 6.3 (dd, 2 H, J = 8.1, 2.2), 5.15 (s, 2 H), 3.8 (s, 6 H), 0.90 (s, 18 H), 0.13 (s, 12 H).

2,6-Dihydroxy-9,10-dihydro-11,12-dicarbomethoxyethenoanthracene (±5). Dimethyl acetylenedicarboxylate (7.2 g, 8.3 mL, 10 equiv, 50 mmol) and pyrogallol (63 mg, 0.5 mm, 1 equiv) were added to a suspension of 2,6-dihydroxyanthracene (1.05 g, 5 mmol, 1 equiv) in 20 mL of dioxane. The mixture was refluxed for 2 days. The dioxane was removed under reduced pressure, and the resulting brown viscous oil was chromatographed on silica, using ether as an eluent: yield 1.05 g (60%) of a yellow foam; R_f 0.45; ¹H NMR (acetone-d_6) δ 7.25 (d, 2 H, J = 7.5), 7.00 (d, 2 H, J = 1.5), 6.50 (dd, 2 H, J = 1.5, 7.5), 3.80 (s, 6 H), 5.50 (s, 2 H); ¹³C NMR (CDCl₃) δ 166.50, 154.05, 147.50, 145.99, 135.04, 124.31, 112.02, 111.02, 52.52, 51.59.

2,6-Dihydroxy-9,10-dihydro-11,12-dicarbomethoxyethenoanthracene (±5). Compound **4** (800 mg, 1.38 mmol) was dissolved in 20 mL of MeOH; 1 mL of CH₂Cl₂ and 1 mL of concentrated HCl were added. The reaction was stirred at room temperature for 6.5 h. The solution was concentrated and chromatographed over flash silica using ether as an eluent to give 450 mg (93%) of a white solid, R_f 0.45. This material could be crystallized from CHCl₃: mp 235–237 °C; NMR as above; MS, *m/e* 352 (M⁺), 293 (100), 278, 261, 249, 234, 210, 181, 152, 59; HRMS 352.0956, calcd for C₂₀H₁₆O₆ 352.0947. Anal. Calcd: C, 68.18; H, 4.58. Found: C, 67.62; H, 4.42.

2,6-Bis(*n*-bromoalkoxy)-9,10-dihydro-11,12-dicarbomethoxyethenoanthracene (6a–c). To a solution of the diol ±5 (704 mg, 2 mmol, 1 equiv) in 35 mL of acetone were added Cs₂CO₃ (3.25 g, 10 mmol, 5 equiv) and the α,ω-dibromoalkane (20 mmol, 10 equiv). The solution was gently refluxed in the dark for 18 h. The cesium salts were removed

by filtration and washed with acetone. The filtrate was concentrated and chromatographed over flash silica using 30% ethyl acetate/petroleum ether as an eluant; yield, 55–70% of a light yellow oil.

6a: ¹H NMR (CDCl₃) δ 7.25 (d, 2 H, J = 7.5), 7.08 (d, 2 H, J = 2.0), 6.50 (dd, 2 H, J = 7.5, 2.0), 5.39 (s, 2 H), 3.95 (t, 4 H, J = 7.0), 3.80 (s, 6 H), 3.50 (t, 4 H, J = 7.0), 2.05 (quintet, 4 H, J = 7.0); ¹³C NMR (CDCl₃) δ 165.76, 156.42, 146.98, 145.72, 135.74, 124.06, 111.46, 109.71, 65.35, 52.24, 51.59, 32.11, 29.90.

6b: ¹H NMR (CDCl₃) δ 7.20 (d, 2 H, J = 7.5), 6.90 (d, 2 H, J = 1.5), 6.45 (dd, 2 H, J = 7.5, 1.5), 5.30 (s, 2 H), 3.90 (t, 4 H, J = 6.1), 3.80 (s, 6 H), 3.40 (t, 4 H, J = 6.1), 1.90 (m, 8 H); ¹³C NMR (CDCl₃) δ 166.56, 157.35, 147.74, 146.43, 136.79, 124.75, 112.13, 110.32, 69.04, 52.99, 52.33, 34.07, 30.01, 28.42.

6c: ¹H NMR (CDCl₃) δ 7.2 (d, 2 H, J = 7.5), 6.9 (d, 2 H, J = 1.5), 6.4 (dd, 2 H, J = 7.5, 1.5), 5.3 (s, 2 H), 3.8 (t, 4 H, J = 7), 3.75 (s, 6 H), 3.3 (t, 4 H, J = 7), 1.9–1.3 (m, 12 H); ¹³C NMR (CDCl₃) δ 166.32, 157.35, 147.73, 146.43, 136.10, 124.66, 112.05, 110.23, 68.25, 52.85, 52.26, 34.33, 32.84, 28.81, 25.23.

2,6-Diethoxy-9,10-dihydro-11,12-dicarbomethoxyethenoanthracene (30). Ethyl iodide (1.1 g, 7.1 mmol, 568 μL) and ±5 (250 mg, 0.71 mmol) were dissolved in 20 mL of acetonitrile in a dry round-bottomed flask. Cs₂CO₃ (925 mg, 2.8 mmol) was added and the reaction stirred at 50 °C for 2 h. The reaction was then filtered, concentrated, and chromatographed (R_f 0.28 in 2/1 isooctane/ethyl acetate) yielding 270 mg of a white foam (93% yield): ¹H NMR (CDCl₃) δ 7.20 (d, 2 H, J = 7.5), 6.90 (d, 2 H, J = 1.5), 6.45 (dd, 2 H, J = 7.5, 1.5), 5.30 (s, 2 H), 3.90 (q, 4 H, J = 6.6), 3.75 (s, 6 H), 1.30 (t, 6 H, J = 6.6); ¹³C NMR (CDCl₃) δ 165.99, 156.82, 147.20, 145.79, 135.51, 124.11, 111.49, 109.75, 63.65, 52.34, 51.77, 14.84.

(9S,10S,11R,12R)- and (9R,10R,11R,12R)-2,6-Bis(*tert*-butyldimethylsiloxy)-9,10-dihydro-11,12-dicarboxyethanoanthracene Bis[(+)-menthyl ester] (21 and 22). Di-(+)-menthyl fumarate (1.79 g, 4.56 mmol, 1 equiv, 4.56 mL of a 1 M solution in toluene) was added to a dry 100-mL flask fitted with a thermometer and an argon inlet. The reaction was then cooled to –45 °C. Diethylaluminum chloride (3.3 g, 27 mmol, 6 equiv, 15.2 mL of a 1.8 M toluene solution) was added over 2 min to the cooled solution, which became orange. After the temperature re-equilibrated, the anthracene **3** (2.00 g, 4.56 mmol, 1 equiv, 11.2 mL of 0.41 M solution in toluene) was added in a slow stream over 10 min, keeping the temperature below –30 °C at all times. After 5 h at –45 °C, the reaction was slowly warmed to 0 °C over 12 h and then carefully poured into 30 mL of chilled toluene stirring over 100 mL of chilled saturated aqueous sodium potassium tartrate (*Caution gas evolution!*). The organic layer and two further toluene extractions of the water were combined, dried (MgSO₄), concentrated, and chromatographed over 100 g of flash silica (3–5% Et₂O in hexane). The mixed fractions containing **21** and **22** were collected (R_f 0.25–0.20; 1.68 g). Anthracene **3** (600 mg, 30%; R_f 0.64) and fractions containing pure **22** (R_f 0.2) were also collected. Mixed **21** and **22** were dissolved in 17 mL of pentane at room temperature and chilled slowly to –100 °C. Pure **21** crystallized from solution (923 mg, 24%; 34% based on recovered starting material). The total yield of Diels–Alder adducts equaled 62%, 89% based on recovered starting material. Syn diastereomer **21:** ¹H NMR (CDCl₃) δ 7.13 (d, 2 H, J = 8), 6.67 (d, 2 H, J = 2), 6.52 (dd, 2 H, J = 2, 8), 4.51 (td, 2 H), 4.49 (s, 2 H), 3.27 (s, 2 H), 1.96 (d septets, 2 H), 1.68, 1.64, 1.37 (m's, 16 H), 0.93, 0.82, 0.72 (3 d, 18 H, J = 7), 0.93 (s, 18 H), 0.12, 0.11 (2 s, 12 H); ¹³C NMR (CDCl₃) δ 171.18, 153.36, 141.42, 134.89, 123.63, 116.90, 116.42, 74.84, 48.52, 47.00, 46.49, 40.77, 34.37, 31.43, 26.24, 25.81, 23.32, 22.13, 21.15, 18.23, 16.28, –4.12, –4.15; [α]_D +13° (*c* 0.4, 0.2, CHCl₃); EI-MS; *m/e* 831 (M⁺), 438 (compound **3**); HRMS 830.5358, calcd for C₅₀H₇₈O₆Si₂ 830.5337. Anti diasteriomer **22:** ¹H NMR (CDCl₃) δ 6.99 (d, 2 H, J = 8), 6.82 (d, 2 H, J = 2), 6.50 (dd, 2 H, J = 2, 8), 4.55 (td, 2 H), 4.51 (s, 2 H), 3.30 (s, 2 H), 1.92 (d septets, 2 H), 1.77, 1.62, 1.36 (m's, 16 H), 0.83 (d, 6 H, J = 7), 0.92, 0.69 (2 d, 12 H, J = 7); 0.95 (s, 18 H), 0.15 (2 s, 12 H); ¹³C NMR (CDCl₃) δ 171.31, 153.55, 143.93, 132.43, 125.14, 116.46, 115.40, 74.80, 48.48, 47.06, 46.49, 40.87, 34.38, 31.49, 26.17, 25.87, 23.31, 22.17, 21.20, 18.34, 16.30, –4.04; [α]_D +58° (*c* 0.2, CHCl₃); EI-MS, 831 (M⁺), 438 (compound **3**).

(9S,10S)- and (9R,10R)-2,6-Dihydroxy-9,10-dihydro-11,12-dicarboxyethenoanthracene Bis[(+)-menthyl ester] (23 and 24). Diels–Alder adduct **21** or **22** (920 mg, 1.11 mmol, 1 equiv) and diphenyl diselenide (553 mg, 1.77 mmol, 1.6 equiv) were placed in a flask and dissolved in 25 mL of toluene. Potassium *tert*-butoxide (348 mg, 3.10 mmol, 2.8 equiv, 2.5 mL of a 1.25 M solution in tetrahydrofuran) was injected into the reaction. After 5 min of stirring at room temperature, 2-propanol (130 mL) was added to the reaction, and all solids dissolved. HCl (37% aqueous, 8 mL) was added and the reaction stirred overnight at room temperature. A white precipitate formed with the addition of the acid. After 18 h, the reaction finished (TLC, 1/1 isooctane/EtOAc).

Ethyl acetate (250 mL), NaHCO₃ (300 mL, saturated aqueous), and 1 M potassium phosphate buffer (pH 7, 100 mL) were added to the reaction. The organic layer and another ethyl acetate extraction of the aqueous layer were combined, dried (MgSO₄), concentrated, and chromatographed (150 g of flash silica, isooctane/ethyl acetate, 1.2/1). With routine air exposure during the extraction procedure the phenyl diselenide was quantitatively recovered (R_f 0.70). Clean fractions of 23 (from 21) or 24 (from 22) were collected (R_f 0.36) yielding an off-white solid (650 mg, 98%).

Compound 24 (from 22): ¹H NMR (CD₃CN) δ 7.15 (d, 2 H, *J* = 8), 6.88 (d, 2 H, *J* = 2), 6.87 (s, 2 H), 6.42 (dd, 2 H, *J* = 2, 8), 5.28 (s, 2 H), 4.75 (td, 2 H), 1.98, 1.81, 1.55, 1.38, 1.31, 0.96 (m's, 18 H), 0.89, 0.88, 0.78 (3 d, 18 H, *J* = 7); ¹³C NMR (CD₃CN, at 1.30 ppm) δ 165.17, 154.91, 147.05, 146.80, 135.55, 124.65, 112.15, 111.16, 76.14, 52.14, 47.60, 41.39, 34.77, 32.06, 26.89, 24.00, 22.26, 20.92, 16.63; [α]_D +35.4° (*c* 3.4, CH₃CN); EI-MS *m/e* 600 (M⁺), 280, 235, 210 (compound 2); HRMS 600.3427, calcd for C₃₈H₄₈O₆ 600.3451. Compound 23 (from 21): ¹H NMR (CD₃CN) δ 7.17 (d, 2 H, *J* = 8), 6.89 (s, 2 H), 6.85 (d, 2 H, *J* = 2), 6.42 (dd, 2 H, *J* = 2, 8), 5.28 (s, 2 H), 4.79 (td, 2 H), 2.02, 1.68, 1.49, 1.40 (m's, 18 H), 0.89, 0.88, 0.78 (3 d, 18 H, *J* = 7); ¹³C NMR (CD₃CN at 1.30 ppm) δ 165.17, 154.90, 146.95, 146.73, 135.54, 124.67, 112.09, 111.11, 76.10, 52.09, 47.57, 41.38, 34.74, 32.04, 26.83, 23.92, 22.25, 20.93, 16.56; [α]_D +65.2° (*c* 2.2, CH₃CN); EI-MS, *m/e* 600 (M⁺), 280, 210 (compound 2); HRMS 600.3439, calcd for C₃₈H₄₈O₆ 600.3451.

(9*S*,10*S*)- and (9*R*,10*R*)-2,6-Dihydroxy-9,10-dihydro-11,12-dicarbomethoxyethenoanthracene [(−)-5 and (+)-5]. Either 23 or 24 (105 mg, 0.175 mmol) was dissolved in methanol (5 mL). Methanesulfonic acid (0.25 mL) was added dropwise to the stirred solution, and the reaction was brought to reflux. The progress of the ester exchange was followed by TLC (Et₂O). After 40 h at reflux, the reaction was cooled to room temperature and mixed with 10 mL each of ethyl acetate and 1 M potassium phosphate buffer (pH 7). The organic layer and another ethyl acetate extraction of the aqueous layer were combined, dried (MgSO₄), and concentrated yielding crude product. Phenol (−)-5 or (+)-5 was purified by crystallization from CHCl₃ in several crops or by flash chromatography (15% petroleum ether in ether, R_f 0.35): yield (chromatography) 57 mg (93%); ¹H NMR (CD₃CN) δ 7.17 (d, 2 H, *J* = 8), 6.86 (s, 2 H), 6.84 (d, 2 H, *J* = 2), 6.41 (dd, 2 H, *J* = 2, 8), 5.32 (s, 2 H), 3.71 (s, 6 H); ¹³C NMR (CD₃CN at 1.30 ppm) δ 166.13, 154.86, 147.64, 146.76, 135.55, 124.74, 112.20, 111.15, 52.76, 51.89; (−)-5 [α]_D −60° (*c* 0.76, CH₃CN), (+)-5 [α]_D +61° (*c* 0.23, CH₃CN); EI-MS, *m/e* 352 (M⁺), 293 (M − CO₂Me), 234, 210; HRMS 352.0939, calcd for C₂₀H₁₆O₆ 352.0947.

Macrocyclizations. The macrocycles (7–12) were prepared in the same way. A flame-dried flask was charged with 1 equiv of ±5 and 1 equiv of the appropriate dibromide 6. DMF was added to make the solution 1 mM in these reactants. Cs₂CO₃ (5 equiv) was added. The flash was protected from light and warmed to 60 °C. The reaction finished in 3–4 days. The DMF was removed under vacuum, and the residue was partitioned between CH₂Cl₂ and 1 N HCl. The organic layer was washed with H₂O and then brine. The organic layer was dried (MgSO₄) and concentrated. The crude reaction mixture was subjected to flash chromatography to isolate the two dimeric macrocycles. This mixture was then separated by preparative reverse-phase HPLC. Listed below are the conditions for all the chromatography and the spectral data for the macrocycles.

Macrocycles 7 and 8: flash chromatography, 50% ethyl acetate/petroleum ether, yield 35%; RPHPLC, 20% H₂O/CH₃OH, 12 mL/min flow rate, t_R(meso) 17.5 min, t_R(*d,l*) 21.9 min; HRMS 784.2524, calcd for C₄₆H₄₀O₁₂ 784.2520.

7: ¹H NMR (CDCl₃) δ 7.03 (d, 4 H, *J* = 8.0), 6.82 (d, 4 H, *J* = 2.5), 6.39 (dd, 4 H, *J* = 8.0, 2.5), 5.17 (s, 4 H), 4.03 (m, 8 H), 3.75 (s, 12 H), 2.03 (m, 4 H); ¹³C NMR (CDCl₃) δ 165.52, 156.37, 146.40, 145.29, 135.27, 123.54, 112.26, 108.96, 63.77, 52.44, 51.67, 29.41; FAB-MS, *m/e* 785 (MH⁺), 753, 725, 309, 155.

8: ¹H NMR (CDCl₃) δ 7.01 (d, 4 H, *J* = 7.1), 6.80 (d, 4 H, *J* = 2.3), 6.39 (dd, 4 H, *J* = 7.1, 2.3), 5.18 (s, 4 H), 3.99 (m, 8 H), 3.74 (s, 12 H), 1.98 (m, 4 H); ¹³C NMR (CDCl₃) δ 165.53, 156.06, 146.48, 145.39, 135.34, 123.63, 111.32, 109.99, 63.51, 52.42, 51.75, 29.55; FAB-MS, *m/e* 785 (MH⁺), 753, 725, 309, 155.

Macrocycles 9 and 10: flash chromatography, 40% ethyl acetate/petroleum ether, yield 51%; RPHPLC, 15% H₂O/CH₃OH, 12 mL/min flow rate, t_R(meso) 18.1 min, t_R(*dl*) 28.8 min; HRMS 812.2812, calcd for C₄₈H₄₄O₁₂ 812.2833.

9: ¹H NMR (CDCl₃) δ 7.10 (d, 4 H, *J* = 8.3), 6.82 (d, 4 H, *J* = 2.44), 6.36 (dd, 4 H, *J* = 8.3, 2.44), 5.22 (s, 4 H), 3.75 (m, 8 H), 3.76 (s, 12 H), 1.69 (m, 8 H); ¹³C NMR (acetone-d₆, CH₂Cl₂) δ 166.19, 157.40, 147.20, 146.58, 136.40, 124.41, 112.30, 110.16, 67.91, 52.33, 51.88, 25.60; FAB-MS, *m/e* 813 (MH⁺), 781, 753, 670, 309, 155, 119.

10: ¹H NMR (CDCl₃) δ 7.10 (d, 4 H, *J* = 8.3), 6.86 (d, 4 H, *J* = 2.4), 6.41 (dd, 4 H, *J* = 8.3, 2.4), 5.25 (s, 4 H), 3.90 (m, 8 H), 3.79 (s, 12 H), 1.78 (m, 8 H); ¹³C NMR (acetone-d₆) δ 166.45, 157.73, 147.75, 147.18, 136.88, 124.85, 112.62, 110.46, 68.15, 52.47, 52.16, 25.72; FAB-MS, *m/e* 813 (MH⁺), 781, 753, 670, 309, 155, 119.

Macrocycles 11 and 12: flash chromatography, 10:1 CHCl₃/Et₂O, yield 40%; RPHPLC, 15% H₂O/CH₃OH, 12 mL/min flow rate, t_R-(meso) 31.3 min, t_R(*dl*) 40 min; HRMS 840.3137, calcd for C₅₀H₄₈O₁₂ 840.3146. Anal. Calcd: C, 71.42; H, 5.75. Found: C, 71.27; H, 5.58.

11: ¹H NMR (CDCl₃) δ 7.07 (d, 4 H, *J* = 8.0), 6.77 (d, 4 H, *J* = 2.1), 6.34 (dd, 4 H, *J* = 8.0, 2.1), 5.21 (s, 4 H), 3.85 (m, 8 H), 3.74 (s, 12 H), 1.67 (m, 8 H), 1.55 (m, 4 H); ¹³C NMR (CDCl₃) δ 166.00, 156.82, 146.94, 145.77, 135.49, 123.93, 111.61, 109.50, 67.68, 52.30, 51.68, 28.43, 22.48; FAB-MS, *m/e* 841 (MH⁺), 809, 781, 698, 361, 293, 210, 119.

12: ¹H NMR (CDCl₃) δ 7.00 (d, 4 H, *J* = 8.1), 6.77 (d, 4 H, *4* = 2.2), 6.29 (dd, 4 H, *J* = 8.1, 2.2), 5.15 (s, 4 H), 3.79 (m, 8 H), 3.69 (s, 12 H), 1.61 (m, 8 H), 1.55 (m, 4 H); ¹³C NMR (CDCl₃) δ 166.01, 156.67, 147.00, 145.79, 135.50, 124.00, 111.35, 109.90, 67.58, 52.31, 51.73, 28.44, 22.50; FAB-MS, *m/e* 841 (MH⁺), 809, 781, 698, 361, 293, 210, 119.

Macrocycles 13–18: (±)5 and Benzylic Dibromides. Racemic ±5 phenol (250 mg, 0.7 mmol, 2 equiv) and cesium carbonate (2.82 g, 7 mmol, 10 equiv) were placed in an oven-dried 1-L flask, while 700 mL of dry DMF was added by cannula. The appropriate α,α′-dibromoxylene (185 mg, 0.7 mmol, 2 equiv) was added and the reaction stirred for 3 days in the dark. Acetic acid (1 mL) and flash silica gel were added to the reaction, and the solvent was stripped under vacuum on a rotary evaporator. The coated silica was placed on a column of 100 g of flash silica and eluted with 15/1–10/1 chloroform/ether. The two dimeric macrocycle diastereomers eluted together at R_f 0.45. Higher oligomers followed at lower R_f. The meso and *d,l* diastereomers were separated and isolated by HPLC, eluting with 5–10% acetonitrile in toluene. Yields are for the combined meso and *d,l* diastereomers.

Enantiomerically Pure Macrocycles (+15, −15, +17, −17, −19). The following general procedure was used. (−)-5 (100 mg, 0.284 mmol, 1 equiv) and α,α′-dibromo-*p*-xylene (75 mg, 0.284 mmol, 1 equiv) or *trans*-1,4-cyclohexanedimethanol ditosylate (90 mg, 0.1991 mmol, 1 equiv) were placed in a dried 100-mL flask and dissolved in 10 mL of anhydrous DMF. This solution, along with two 5-mL rinsings of the flask were drawn into a 30-mL syringe, and this syringe was placed in a syringe pump. Clean DMF (20 mL) and cesium carbonate (0.46 g, 1.42 mmol, 5 equiv) were added to the reaction flask, and the addition was started so that the solution would be added to the reaction at ≈0.45 mL/h (total addition time 45 h). This reaction was run in the dark and stirred rapidly. Twelve hours after the addition finished, the reaction was filtered and the DMF evaporated. The crude products were purified by chromatography (15, 17, 25–27; 5% EtOAc/CHCl₃).

Where racemic and enantiomerically pure materials were synthesized, spectral data for the racemate are reported. Optical rotations are given for the enantiomerically pure molecules synthesized by the syringe pump procedure. Higher oligomer yields are from macrocyclizations with one enantiomer of 5.

13: ¹H NMR (CDCl₃) 7.46, 7.39 (AA′BB′, 8 H), 7.14 (d, 4 H, *J* = 8), 6.96 (d, 4 H, *J* = 2), 6.51 (dd, 4 H, *J* = 2, 8), 5.26 (s, 4 H), 4.91 (AB, *J* = 10.2, Δv = 48.2 Hz, 8 H), 3.76 (s, 12 H); ¹³C NMR (CDCl₃) δ 165.92, 156.74, 146.84, 145.72, 136.30, 135.51, 130.50, 128.99, 124.18, 111.92, 111.04, 69.10, 52.38, 51.68; FAB-MS, *m/e* 909 (M + 1), 877 (M − OCH₃), 849 (M − CO₂Me), 766 (M − DMAD), 613, 395, 309, 155, 119; HRMS 908.2792, calcd for C₅₆H₄₄O₁₂ 908.2833.

14: ¹H NMR (CDCl₃) δ 7.46, 7.38 (AA′BB′, 8 H), 7.14 (d, 4 H, *J* = 8), 6.94 (d, 4 H, *J* = 2), 6.55 (dd, 4 H, *J* = 2, 8), 5.26 (s, 4 H), 4.93 (AB, *J* = 10.4, Δv = 41.2 Hz, 8 H), 3.76 (s, 12 H); ¹³C NMR (CDCl₃) δ 165.94, 156.70, 146.84, 145.71, 136.26, 135.52, 130.38, 128.96, 123.97, 112.19, 110.54, 69.06, 52.38, 51.67; FAB-MS, *m/e* 909 (M + 1), 877 (M − OCH₃), 849 (M − CO₂Me), 766 (M − DMAD), 613, 395, 309, 155, 119; HRMS 908.2801. Combined yield of the two *o*-xylyl diastereomers was 24%.

15: ¹H NMR (CDCl₃) δ 7.37–7.16 (m, 8 H), 7.08 (d, 4 H, *J* = 8), 6.95 (d, 4 H, *J* = 2), 6.37 (dd, 4 H, *J* = 2, 8), 5.27 (s, 4 H), 4.99 (s, 8 H, benzene-d₆ δ 4.47; AB, 8 H, *J* = 14.3, Δv = 59.3 Hz), 3.77 (s, 12 H); ¹³C NMR (CDCl₃) δ 165.97, 156.50, 147.09, 145.78, 137.70, 135.92, 128.67, 126.20, 125.53, 124.15, 111.60, 110.50, 69.88, 52.35, 51.67; FAB-MS; *m/e* 909 (M + 1), 877 (M − OCH₃), 849 (M − CO₂Me), 817, 766 (M − DMAD), 309, 155, 119; HRMS 908.2810; (−)-15a [α]_D −51° (*c* 3.2 in CH₃CN), (+)-15a [α]_D +58° (*c* 1.0, CH₃CN).

16: ¹H NMR (CDCl₃) δ 7.38–7.20 (m, 8 H), 7.10 (d, 4 H, *J* = 8), 6.93 (d, 4 H, *J* = 2), 6.35 (dd, 4 H, *J* = 2, 8), 5.24 (s, 4 H), 4.91 (AB, 8 H, *J* = 11.2, Δv = 68.3 Hz), 3.75 (s, 12 H); ¹³C NMR (CDCl₃) δ 165.95, 156.52, 147.03, 145.71, 137.63, 135.81, 128.72, 126.08, 125.11,

124.07, 112.11, 109.36, 69.93, 52.36, 51.61; FAB-MS, m/e 909 (M + 1) 877 (M – OCH$_3$), 849 (M – CO$_2$Me), 817, 766 (M – DMAD), 309, 275, 155, 119; HRMS 908.2784. Combined yield of the two m-xylyl diastereomers was 36%.

Trimer 26: R_f 0.22; yield 14%; [^1]H NMR (CDCl$_3$) δ 7.36–7.27 (m, 12 H), 7.18 (d, 6 H, J = 8), 7.00 (d, 6 H, J = 2), 6.50 (dd, 6 H, J = 2, 8), 5.29 (s, 6 H), 4.94 (s, 12 H), 3.75 (s, 18 H); [^13]C NMR (CDCl$_3$) δ 165.46, 156.34, 146.72, 145.51, 147.14, 135.75, 128.49, 126.77, 126.40, 123.91, 111.85, 110.00, 70.28, 52.41, 51.91; (+)-26 [α]$_D$ +19° (c 1.7, CH$_3$CN), (–)-26 [α]$_D$ –20° (c 1.0, CH$_3$CN).

Tetramer (+)-27: R_f 0.15; yield 7%; [^1]H NMR (CDCl$_3$) δ 7.42–7.35 (m, 16 H), 7.25 (d, 8 H, J = 8), 7.08 (d, 8 H, J = 2), 6.58 (dd, 8 H, J = 2, 8), 5.46 (s, 8 H), 5.02 (s, 16 H), 3.81 (s, 24 H); [^13]C NMR (CDCl$_3$) δ 165.44, 156.31, 146.76, 145.49, 137.33, 135.72, 128.49, 126.54, 125.90, 123.92, 111.82, 110.01, 70.15, 52.40, 51.90; [α]$_D$ +65° (c 1.0, CH$_3$CN); FAB-MS, m/e 1819 (M + 3), 1742, 1679, 1518.

17: [^1]H NMR (CDCl$_3$) δ 7.19 (s, 8 H), 7.06 (d, 4 H, J = 8), 6.88 (d, 4 H, J = 2), 6.37 (dd, 4 H, J = 2, 8), 5.21 (s, 4 H), 5.06 (AB, 8 H, J = 13.6, Δυ = 53.5 Hz), 3.75 (s, 12 H); [^13]C NMR (CDCl$_3$) δ 165.95, 156.24, 146.97, 145.66, 136.84, 135.76, 126.71, 123.92, 112.44, 109.92, 69.62, 52.35, 51.56; FAB-MS, m/e 909 (M + 1), 877 (M – OCH$_3$), 849 (M – CO$_2$Me), 766 (M – DMAD), 309, 155, 119; HRMS 908.2853; (+)-17a [α]$_D$ +144° (c 1.1, CH$_3$CN), (–)-17a [α]$_D$ –144° (c 1.7, CH$_3$CN).

18: [^1]H NMR (CDCl$_3$) δ 7.28 (m, 8 H), 7.14 (d, 4 H, J = 8), 6.96 (d, 4 H, J = 2), 6.45 (dd, 4 H, J = 2, 8), 5.27 (s, 4 H), 4.97 (AB, 8 H, J = 12.6, Δυ = 28.2 Hz), 3.75 (s, 12 H); [^13]C NMR (CDCl$_3$) δ 165.94, 156.33, 146.99, 145.66, 136.96, 135.78, 126.43, 123.95, 112.65, 109.80, 69.72, 52.36, 51.57; FAB-MS, m/e 909 (M + 1), 877 (M – OCH$_3$), 849 (M – CO$_2$Me), 766 (M – DMAD), 309, 155, 119; HRMS 908.2766. Combined yield of the two p-xylyl diastereomers was 18%.

Trimer (+)-25: [^1]H NMR (CDCl$_3$) δ 7.28 (s, 12 H), 7.14 (d, 6 H, J = 8), 6.96 (d, 6 H, J = 2), 6.45 (dd, 6 H, 4 = 2, 8), 5.27 (6 H), 4.98 (AB, 12 H, J = 12.4, Δυ = 27.6 Hz), 3.75 (s, 18 H); [^13]C NMR (CDCl$_3$) δ 165.48, 156.06, 146.74, 145.46, 136.43, 135.63, 127.07, 123.89, 111.86, 109.92, 69.77, 52.44, 51.86; [α]$_D$ 17.7° (c 0.4, CH$_3$CN); FAB-MS, m/e 1363 (M + 1), 1299, 1220.

19: The product 19 plus higher molecular weight materials were isolated by flash chromatography using 5% Et$_2$O/CHCl$_3$ as an eluent. The individual cyclic oligomers could be isolated by preparative TLC with multiple elutions using 1% Et$_2$O/CHCl$_3$ as eluent. The highest R_f material was the dimer with the higher homologues running progressively slower. **19:** 5 mg (5.5% yield); [^1]H NMR (CDCl$_3$) δ 7.09 (d, 4 H, J = 8.05), 6.82 (d, 4 H, J = 2.20), 6.38 (dd, 4 H, J = 8.05, 2.20), 5.20 (s, 4 H), 3.86 (dd, 4 H, J = 5.86, 10.98), 3.73 (s, 12 H), 3.71 (dd, 4 H, J = 5.86, 10.98), 1.60 (m, 12 H), 0.85 (m, 8 H); [^13]C NMR (CDCl$_3$) δ 165.97, 156.61, 146.93, 145.82, 135.68, 123.79, 112.16, 110.66, 73.62, 52.25, 51.72, 36.45, 28.46; [α]$_D$ –44° (c 0.12, CH$_3$CN). Some presumed trimer 28 and tetramer 29 could be isolated.

Trimer 28: 2.5 mg; [^1]H NMR (CDCl$_3$) δ 7.18 (d, 6 H, J = 8.1), 6.88 (d, 6 H, J = 2.2), 6.42 (dd, 6 H, J = 8.1, 2.2), 5.24 (s, 6 H), 3.74 (s, 18 H), 3.68 (m, 12 H), 1.60 (m, 36 H), 0.85 (m, 24 H); [α]$_D$ –8.4° (c 0.154, CH$_3$CN).

Tetramer 29: 0.8 mg; [^1]H NMR (CDCl$_3$) δ 7.17 (d, 8 H, J = 8.1), 6.90 (d, 8 H, J = 2.2), 6.43 (dd, 8 H, J = 8.1, 2.2), 5.26 (s, 8 H), 3.76 (s, 24 H), 3.66 (m, 16 H), 1.60 (m, 48 H), 0.85 (m, 32 H); [α]$_D$ +28° (c 0.08, CH$_3$CN).

Ester Hydrolysis Conditions. All the macrocycles were hydrolyzed in a similar manner. The tetraesters (7–19) were dissolved in either DMSO or THF, and then CsOH (8–10 equiv) was added. Five percent (v/v) water was added and the reaction stirred overnight. The solution was lyophilized and the resulting solid dissolved in a minimum amount of H$_2$O. The aqueous solution was added to the top of a cation-exchange column (neutral pH, Dowex 50 × 4, NH$_4$$^+$ form) and the material eluted with doubly distilled water. The fractions containing the host(s) were determined by their UV activity on reverse-phase TLC. The samples were combined and lyophilized to give the free acids. Standard solutions of these hosts were made by adding the appropriate amount of CsOD and diluting with buffer to a specified volume. Typical yields were 75–90%. The hosts are characterized below.

III$_{meso}$: [^1]H NMR (borate-d, external TSP at 0.00 ppm) δ 7.09 (d, 4 H, J = 8.3), 7.01 (d, 4 H, J = 2.4), 6.50 (dd, 4 H, J = 8.3, 2.4), 5.14 (s, 4 H), 4.22 (m, 4 H), 4.11 (m, 4 H), 2.05 (m, 4 H); [^13]C NMR (borate-d, external TSP at 0.00 ppm) δ 172.23, 153.27, 145.49, 144.68, 135.82, 121.86, 109.03, 107.97, 62.61, 50.31, 26.94.

III$_{dl}$: [^1]H NMR (borate-d, external TSP at 0.00 ppm) δ 7.21 (d, 4 H, J = 8.05), 7.05 (d, 4 H, J = 2.2), 6.60 (dd, 4 H, J = 8.1, 2.2), 5.20 (s, 4 H), 4.22 (m, 8 H), 2.05 (m, 4 H); [^13]C NMR (DMSO-d$_6$, D$_2$O) δ 170.04, 159.91, 149.20, 148.48, 139.73, 125.54, 118.89, 112.89, 66.41, 53.60, 29.87.

IV$_{meso}$: [^1]H NMR (CD$_3$OD) δ 7.00 (d, 4 H, J = 8.0), 6.94 (d, 4 H, J = 2.2), 6.43 (dd, 4 H, J = 8.0, 2.2), 5.46 (s, 4 H), 3.88 (m, 8 H), 1.75 (m, 8 H); [^13]C NMR (CD$_3$OD) δ 168.38, 157.55, 149.18, 147.06, 136.90, 124.73, 112.08, 111.07, 68.13, 53.49, 25.58.

IV$_{dl}$: [^1]H NMR (CD$_3$CN) δ 7.08 (d, 4 H, J = 8.0), 6.92 (d, 4 H, J = 1.7), 6.38 (dd, 4 H, J = 8.0, 1.7), 5.60 (s, 4 H), 3.8 (m, 8 H), 1.7 (m, 8 H); [^13]C NMR (CD$_3$OD) δ 168.79, 157.33, 151.05, 147.43, 137.57, 124.51, 112.15, 111.37, 68.61, 54.23, 26.04.

V$_{meso}$: [^1]H NMR (D$_2$O, phosphate buffer[^35]) δ 7.12 (d, 4 H, J = 2.2), 6.97 (d, 4 H, J = 8.0), 6.20 (dd, 4 H, J = 8.0, 2.2), 5.23 (s, 4 H), 3.98 (m, 4 H), 3.82 (m, 4 H), 1.58 (m, 8 H), 1.45 (m, 4 H); [^13]C NMR (D$_2$O) δ 173.79, 154.37, 146.81, 146.25, 137.70, 123.16, 111.68, 110.09, 68.36, 57.92, 26.74, 21.04.

V$_{dl}$: [^1]H NMR (D$_2$O, phosphate buffer[^35]) δ 7.04 (d, 4 H, J = 8.0), 6.87 (d, 4 H, J = 2.2), 6.30 (dd, 4 H, J = 8.0, 2.2), 5.10 (s, 4 H), 3.68 (m, 8 H), 1.26 (m, 8 H), 1.10 (m, 4 H); [^13]C NMR (D$_2$O) δ 171.95, 152.61, 145.00, 144.49, 136.09, 121.42, 110.26, 108.81, 66.94, 50.07, 24.62, 19.11.

O$_{meso}$: [^1]H NMR (D$_2$O, external TSP-d$_4$ at 0.00 ppm) δ 7.43, 7.30 (AA'BB', 8 H), 7.01 (d, 4 H, J = 8), 6.98 (d, 4 H, J = 2), 6.57 (dd, 4 H, J = 2, 8), 5.73 (s, 4 H), 4.94 (AB, J = 11.1, Δυ = 16.2 Hz, 8 H); [^13]C NMR (D$_2$O, external TSP-d$_4$ at 0.00 ppm) δ 165.27, 155.43, 149.10, 146.58, 137.13, 135.42, 129.25, 127.94, 123.32, 111.57, 109.56, 68.50, 52.35.

O$_{dl}$: [^1]H NMR (D$_2$O, external TSP-d$_4$ at 0.00 ppm) δ 7.57 (AA'BB', 8 H), 7.19 (d, 4 H, J = 8), 7.16 (d, 4 H, J = 2), 6.59 (dd, 4 H, J = 2, 8), 5.20 (s, 4 H), 5.10 (AB, J = 11, Δυ = 113 Hz, 8 H).

M$_{meso}$: [^1]H NMR (D$_2$O, external TSP-d$_4$ at 0.00 ppm) δ 6.72 + 5.76 (s + br s, 8 H), 7.14 (d, 4 H, J = 8), 6.77 (d, 4 H, J = 2), 6.11 (dd, 4 H, J = 2, 8), 5.15 (s, 4 H), 3.96 (AB J = 14, Δυ = 99 Hz, 8 H); [^13]C NMR (D$_2$O, external TSP-d$_4$ at 0.00 ppm) δ 174.62, 155.09, 147.75, 147.29, 138.86, 136.80, 128.50, 125.31, 134.03, 123.52, 112.83, 111.59, 70.05, 52.92.

M$_{dl}$, M$_d$, M$_l$: [^1]H NMR (borate-d buffer, external TSP-d$_4$ at 0.00 ppm) δ 7.02 (s + br s, 8 H), 7.26 (d, 4 H, J = 8), 6.97 (d, 4 H, J = 2), 6.44 (dd, 4 H, J = 2, 8), 5.26 (s, 4 H), 4.9 (AB, J = 15, 8 H); [^13]C NMR (D$_2$O, external TSP-d$_4$ at 0.00 ppm) δ 175.38, 155.56, 148.27, 147.66, 139.42, 137.29, 128.95, 125.81, 124.46, 124.19, 113.26, 112.13, 70.33, 52.97; M$_l$ [α]$_D$ –37° (c 0.051, borate-d), M$_d$ [α]$_D$ (S,S,S,S) +37° (c 0.036, borate-d).

P$_{meso}$: [^1]H NMR (D$_3$, external TSP-d$_4$ at 0.00 ppm) δ 7.14 (s, 8 H), 7.13 (d, 4 H, J = 8), 7.04 (d, 4 H, J = 2), 6.38 (dd, 4 H, J = 2, 8), 5.19 (s, 4 H), 5.02 (AB, 8 H); [^13]C NMR (D$_2$O, external TSP-d$_4$ at 0.00 ppm) δ 174.64, 155.00, 147.65, 146.96, 139.08, 136.57, 127.59, 123.88, 113.77, 112.01, 71.69, 52.73.

P$_{dl}$, P$_d$, and P$_l$: [^1]H NMR (D$_2$O, external TSP-d$_4$ at 0.00 ppm) δ 7.21 (s, 8 H), 7.04 (d, 4 H, J = 8), 6.84 (d, 4 H, J = 2), 6.40 (dd, 4 H, J = 2, 8), 5.60 (s, 4 H), 5.02 (AB, J = 13.5, Δυ = 39.3 Hz, 8 H); [^13]C NMR (D$_2$O, external TSP-d$_4$ at 0.00 ppm) δ 176.08, 154.49, 148.59, 146.75, 136.86, 136.29, 126.60, 123.09, 111.69, 109.04, 68.43, 52.34; P$_l$ [α]$_D$ –364° (c 0.021, borate-d), P$_d$ [α]$_D$ +358° (c 0.058, borate-d).

C$_l$: [^1]H NMR (borate-d, external TSP at 0.00 ppm) δ 7.27 (d, 4 H, J = 8.1), 7.05 (d, 4 H, J = 2.2), 6.57 (dd, 4 H, J = 8.1, 2.2), 5.27 (s, 4 H), 3.83 (m, 8 H), 1.66 (m, 12 H), 0.72 (m, 8 H); [^13]C NMR (DMSO-d$_6$/D$_2$O) δ 169.80, 157.01, 148.14, 147.45, 139.81, 125.18, 113.55, 112.31, 75.80, 53.70, 37.43, 29.44; [α]$_D$ –133° (c 0.0372, borate-d).

2,6-Diethoxy-9,10-dihydro-11,12-dicarboxyethenoanthracene bis(cesium salt) (31): [^1]H NMR (borate-d, external TSP at 0.00 ppm) δ 7.31 (d, 2 H, J = 8.3), 7.06 (d, 2 H, J = 2.4), 6.55 (dd, 2 H, J = 8.3, 2.4), 5.28 (s, 2 H), 4.00 (dq, 4 H, J = 7.1), 1.30 (t, 6 H, J = 7.1); [^13]C NMR (borate-d) δ 172.41, 153.33, 145.60, 144.75, 136.15, 121.74, 109.12, 108.10, 62.69, 50.03, 11.80.

Guests. G1–G8, G14, G16, G19, G20, and G26 were obtained from commercial sources. We synthesized the other trimethylammonium (TMA) guests by exhaustively methylating (5 equiv of CH$_3$I) a DMF or acetonitrile solution of the precursor amine (1 M) overnight, at room temperature. Excess potassium carbonate was added to react with liberated acid when necessary. The reactions were filtered and concentrated. Chloroform was added to dissolve the product and precipitate inorganics. The chloroform solution was filtered, and ether was added to the filtrate precipitating the product.

The tetrafluoroborate salts were prepared by the action of Meerwein's reagent on the dimethylamino precursors in CH$_2$Cl$_2$. Addition of MeOH, concentration of the mixture, and trituration with Et$_2$O gave the crude products. These salts were recrystallized prior to use. The guests were recrystallized from the solvent indicated.

(4-Nitrobenzyl)trimethylammonium Iodide–G15. The product was crystallized from CH$_3$CN/Et$_2$O: [^1]H NMR (borate-d buffer) δ 8.39 (d, 2 H, J = 7.0), 7.82 (d, 2 H, J = 7.0), 4.65 (s, 2 H), 3.17 (s, 9 H); [^13]C

NMR (DMSO-d_6/D$_2$O) δ 150.06, 135.25, 135.21, 125.31, 69.44, 54.28.

(S)-Naphthylethyltrimethylammonium iodide-(-)-G17: prisms from toluene/acetonitrile; ^{1}H NMR (D$_2$O) δ 8.17 (1 H), 7.58, 7.49 (2 t, 1 H each), 7.88 (d, 1 H), 7.92 (d, 1 H), 7.51 (t, 1 H), 7.72 (d, 1 H), 5.54 (q, 1 H), 2.91 (s, 9 H), 1.74 (d, 3 H); ^{13}C NMR (CDCl$_3$) δ 132.27, 131.25, 130.37, 128.12, 127.78, 127.35, 126.96, 125.43, 123.97, 123.00, 66.92, 51.45, 16.54; [α]$_D$ −47° (c 0.16, borate-d).

(R)-Naphthylethyltrimethylammonium iodide-(+)-G17: prisms from toluene/acetonitrile; ^{1}H NMR (D$_2$O) δ 8.17 (d, 1 H), 7.57, 7.49 (2 t, 1 H each), 7.87 (d, 1 H), 7.92 (d, 1 H), 7.50 (t, 1 H), 7.71 (d, 1 H), 5.54 (q, 1 H), 2.91 (s, 9 H), 1.74 (d, 3 H); ^{13}C NMR (CDCl$_3$) δ 133.42, 131.88, 131.07, 128.32, 127.79, 127.71, 126.12, 124.46, 123.63, 123.04, 67.57, 52.05, 17.10; [α]$_D$ +44° (c 0.11, borate-d).

Phenyltrimethylammonium tetrafluoroborate-G11: crystallized from CH$_3$CN/Et$_2$O; ^{1}H NMR (borate-d) δ 7.83 (br d, 2 H), 7.64 (m, 3 H), 3.65 (s, 9 H). Anal. Calcd: C, 48.47; H, 6.33; N, 6.27. Found: C, 48.41; H, 6.53; N, 6.27.

(4-tert-Butylphenyl)trimethylammonium tetrafluoroborate-G12: crystallized from CH$_3$CN/Et$_2$O; ^{1}H NMR (borate-d) δ 7.75 (d, 2 H, J = 7.0), 7.70 (d, 2 H, J = 7.0), 3.63 (s, 9 H), 1.34 (s, 9 H). Anal. Calcd: C, 55.93; H, 7.94; N, 5.02. Found: C, 55.61; H, 7.94; N, 4.99.

1,4-Bis(trimethylammonium)benzene bis(tetrafluoroborate)-G13: crystallized from CH$_3$CN; ^{1}H NMR (borate-d) δ 8.14 (s, 4 H, 3.71 (s, 18 H). Anal. Calcd: C, 39.17; H, 6.14; N, 7.61. Found: C, 39.07; H, 6.14; N, 7.34.

Cyclohexyltrimethylammonium iodide-G18: plates from aqueous acetone; ^{1}H NMR (CD$_3$CN) δ 3.18 (tt, 1 H, J = 3, 12), 2.92 (s, 9 H), 2.08 (dd, 2 H, J = 2, 12), 1.82 (dd, 2 H, J = 2, 13), 1.54 (dt, 1 H, 4 = 2, 14), 1.36 (dq, 2 H, J = 2, 14), 1.22 (tq, 2 H, J = 2, 14), 1.03 (qt, 1 H, J = 2, 14); ^{13}C NMR (borate-d, external TSP-d$_4$ at 0.00 ppm) δ 56.77, 33.10 (t, J = 4), 8.28, 7.27, 6.61.

1-Naphthyltrimethylammoniummethyl Iodide-G25. The product was formed in 82% yield and was recrystallized from CH$_3$CN: ^{1}H NMR (borate-d) δ 8.28 (d, 1 H, J = 10.6), 8.17 (d, 1 H, J = 10.6), 8.09 (d, 1 H, J = 10.6), 7.74 (mt, 1 H), 7.67 (t, 2 H, J = 10.6), 5.06 (s, 2 H), 3.16 (s, 9 H); ^{13}C NMR (DMSO/D$_2$O) δ 135.1, 133.3, 130.7, 129.3, 128.1, 126.8, 124.8, 124.6, 66.9, 54.6.

Adamantyltrimethylammonium iodide (ATMA)-G10: needles from CH$_3$CN; ^{1}H NMR (borate-d, external TSP-d$_4$ at 0.00 ppm) δ 2.99 (s, 9 H), (s, 6 H, 2.07), 2.31 (s, 3 H), 1.70 (AB, 6 H, J = 14, Δv = 31.8 Hz); ^{13}C NMR (CDCl$_3$) δ 73.16, 48.85, 35.29, 35.14, 30.21.

N-Methylisoquinolinium iodide-G9: needles from acetone/water; ^{1}H NMR (CD$_3$CN) δ 9.95 (s, 1 H), 8.76–8.34 (m's, 6 H), 5.10 (s, 3 H); ^{13}C NMR (CDCl$_3$) δ 150.25, 137.30, 137.08, 135.32, 131.42, 130.78, 127.10, 126.10, 48.97.

(-)-Bornyltrimethylammonium iodide bornyl-TMA-G21: ^{1}H NMR (borate-d) δ 3.61 (dd, 1 H), 3.05 (dd, 9 H), 2.21, 1.77, 1.71, 1.46, 1.21 (m's, 7 H), 1.01, 0.90, 0.86 (3s, 3 H each); ^{13}C NMR (CDCl$_3$) δ 82.01, 54.7 (br), 52.35, 51.60, 43.17, 31.58, 28.47, 27.89, 19.89, 19.83, 19.60, 17.48; [α]$_D$ −8.0° (c 0.075, in borate-d).

(S)-(cis)-Myrtanyl-TMA-G22: plates from acetonitrile; ^{1}H NMR (CDCl$_3$) δ 3.78 (dd, 1 H), 3.56 (br d, 1 H), 3.22 (s, 9 H), 2.59, 2.43, 1.86, 1.10 (m's, 11 H), 1.86, 0.94 (s, 3 H each); ^{13}C NMR (CDCl$_3$) δ 76.88, 53.94, 53.82, 47.74, 40.39, 38.30, 35.77, 27.40, 25.75, 23.82, 23.39; [α]$_D$ +23° (c 0.10, borate-d).

(1S,2R)-(1-Methyl-2-phenyl-2-hydroxy)ethyltrimethylammonium iodide [(-)-dimethylephedrine]-G23: ^{1}H NMR (D$_2$O) δ 7.45 (d, 2 H), 7.39 (t, 2 H), 7.31 (t, 1 H), 5.62 (d, 1 H), 4.43 (d, 1 H), 3.60 (q, 1 H), 3.24 (s, 9 H), 1.16 (dt, 1:1:1, 3 H); ^{13}C NMR (CD$_3$CN at 1.3 ppm) δ 141.47, 128.80, 128.19, 126.29, 75.22, 69.39, 53.23 (1:1:1, t, J = 4.4), 7.65; [α]$_D$ −22° (c 0.12, borate-d).

(R)-α-Trimethylammoniumethyl-3,4-dimethoxybenzyl alcohol iodide salt (tetramethylepinephrine)-G24: needles from acetonitrile; cesium carbonate was used instead of K$_2$CO$_3$ for the alkylation reaction; ^{1}H NMR (borate-d, external TSP-d$_4$ at 0.00 ppm) δ 7.09 (m, 3 H), 5.36 (d, 1 H), 3.96 (s, 3 H), 3.88 (s, 3 H), 3.69 + 3.51 (2 dd, 2 H), 3.29 (s, 9 H); ^{13}C NMR (CD$_3$CN at 1.3 ppm) δ 141.24, 132.93, 118.63, 114.65, 111.83, 110.26, 71.04, 68.45, 53.66, 56.11, 54.97; [α]$_D$ +33° (c 0.15, borate-d).

A Macrocyclic Tetraether Bolaamphiphile and an Oligoamino α,ω-Dicarboxylate Combine To Form Monolayered, Porous Vesicle Membranes, Which Are Reversibly Sealed by EDTA and Other Bulky Anions

Jürgen-Hinrich Fuhrhop,* Ulrich Liman, and Volker Koesling

Contribution from the Institut für Organische Chemie der Freien Universität Berlin, Takustrasse 3, 1000 Berlin 33, West Germany. Received February 10, 1988

Abstract: The hydrophobic tetraether macrocycle 1,20-disulfonyl-4,17,23,36-tetraoxacyclooctatriacontane is obtained in the gram scale from 2,2-dithioethanol and 1,12-dodecanediol. Oxidation or methylation of the sulfur atoms leads to bolaamphiphiles which vesiculate on ultrasonication. These amphiphiles are simple analogues of the membrane constituents of *archaebacteria*. The vesicles are acid stable and entrap metal ions (Li$^+$, Fe^{2+}) as well as fluorescent dyes (pyranine, calcein). The dipotassium salt of 2,19-dimethyl-3,6,9,12,15,18-hexaazaeicosanedicarboxylate introduces pores for metal ions into the membrane, but not for the organic dyes. The cationic pores could be closed with water-soluble bulky anions such as camphorsulfonic acid, taurine, and EDTA. The EDTA stopper was extracted from the pore by an excess of Fe(II) ions. Excess EDTA reclosed the pore. This cycle could be repeated several times.

Water-insoluble amphiphiles with head groups on both ends of a hydrophobic chain have been named "bolaamphiphiles". The self-organization of bolaamphiphiles in aqueous media may produce planar or spherical monolayered membranes.[1,2] The

thickness of the hydrophobic membranes is identical with the length of the bipolar amphiphiles and may be as thin as 1.5 nm.[3] Within the hydrophobic membrane, guest amphiphiles of similar lengths and containing a hydrophobic edge ("edge amphiphiles") self-organize to form "domains". The core of these domains is

(1) Gliozzi, A.; Bruno, S.; Basak, T. K.; de Rosa, M.; Gambacorta, A. *Syst. Appl. Microbiol.* **1986,** *7,* 266–271.

(2) Fuhrhop, J.-H.; Fritsch, D. *Acc. Chem. Res.* **1986,** *19,* 130–137.

(3) Fuhrhop, J.-H.; David, H. H.; Mathieu, J.; Liman, U.; Winter, H.-J.; Boekema, E. *J. Am. Chem. Soc.* **1986,** *108,* 1785–1791.